

Spatial and temporal heterogeneity of soil respiration in a bare-soil Mediterranean olive grove

Sergio Aranda-Barranco^{1,2}, Penélope Serrano-Ortiz^{1,2}, Andrew S. Kowalski^{2,3}, Enrique P. Sánchez-Cañete^{2,3}

5 ¹ Department of Ecology, University of Granada, 18071 Granada, Spain.

² Andalusian Institute for Earth System Research (CEAMA-IISTA), University of Granada, 18006 Granada, Spain

³ Department of Applied Physics, University of Granada, 18071 Granada, Spain

Correspondence to: Sergio Aranda-Barranco (sergioaranda@ugr.es)

Abstract. Soil respiration (R_s) is an important carbon flux in terrestrial ecosystems, and knowledge about this CO_2 release process and the drivers involved is a key topic in the context of global change. However, temporal and spatial variability has not been extensively studied in semi-arid systems such as olive groves. In this study, we show a full year of continuous measurements of R_s with six automatic chambers in a fertirrigated olive grove with bare soil in the Mediterranean accompanied by modelled ecosystem respiration (R_{eco}) estimated by decomposing net ecosystem carbon exchange (NEE) measured using eddy covariance (EC) technique. To study spatial variability, the automatic chambers were distributed equally under the canopy (R_s Under-Tree) and in the center of the alley (R_s Alley), and the gradient of R_s between both locations was measured in several manual campaigns in addition to angular changes about the olive trees. The results indicate that R_s Under-Tree was three times larger than R_s Alley in the annual computations. Higher R_s was found on the south face, and an exponential decay of R_s was observed until the alley's center was reached. These spatial changes were used to weigh and project R_s to the ecosystem scale, whose annual balance was 1.6 – 2.3 higher than R_{eco} estimated using EC-derived models. R_s Under-Tree represented 39% of the R_s of the olive grove. We found values of $Q_{10} < 1$ in the vicinity of the olive tree in the warm period. Outbursts of CO_2 emissions associated with precipitation events were detected, especially in the alley, during dry periods, and after extended periods without rain, but were not accurately detected by EC-derived respiration models. We point out an interaction between several effects that vary in time and are different under the canopy than in the alleys that the accepted models to estimate Q_{10} and R_{eco} do not consider. These results show a high spatial and temporal heterogeneity in soil respiration and the factors involved, which must be considered in future works in semi-arid agrosystems.

1 Introduction

Soil respiration (R_s) commonly refers to the natural release of CO_2 from the soil surface into the atmosphere and plays a key role in the carbon cycle. The global annual release of CO_2 through R_s is $\sim 95 \text{ PgC yr}^{-1}$ (Xu and Shang, 2016; Zhao et al., 2017), which is approximately ten times higher than current emissions from fossil fuels (Friedlingstein et al., 2022). Globally, R_s is the second largest carbon flux, accounting for 85%–90% of gross primary production (Hashimoto et al., 2015; Jian et al., 2021). However, global R_s is not constant but has been increasing by 0.04 PgC yr^{-1} between 1960 and 2012 (Zhao et al., 2017).

35 R_s is composed of heterotrophic and autotrophic respiration. R_s is influenced mainly by the carbon supply, temperature, and soil moisture (Hursh et al., 2017), and these parameters vary unevenly with global change. In fact, annual R_s trends respond differently depending on latitude and biome, increasing mainly in boreal zones and decreasing in tropical areas (Lei et al., 2021). In contrast, in semi-arid regions such as the Mediterranean, no long-term trends are observed although reduced rainfall in this region is expected to reduce R_s (Talmon et al., 2011) due to water limitation.

40 The importance of water as a limiting factor on R_s is more complex than previously thought (Leon et al., 2014). The Mediterranean climate is distinguished by irregular rainfall patterns, high evaporation rates, and water scarcity during summer months. These characteristics can drive high temporal variation in R_s because of its critical sensitivity to soil moisture. Water controls the movement of soluble substrates when moisture is scarce, and availability of oxygen when it is abundant (Skopp et al., 1990). However, although R_s has an important influence on the carbon cycle feedback in Mediterranean ecosystems, the understanding of R_s in semi-arid regions is still evolving (González-Ubierna and Lai, 2019). Since heterotrophic R_s is positively correlated with soil organic carbon content (Lei et al., 2021), which is generally low in Mediterranean ecosystems (Muñoz-Rojas et al., 2012), low values of R_s are expected in such ecosystems. However, higher R_s values are found in 45 croplands in which carbon and water respond to management (Wollenberg et al., 2016). More productivity is expected in cropland because of the increase in nutrients provided by fertilizers, soil aeration, and irrigation. Therefore, the conversion to cropland of ecosystems typical of semi-arid areas can increase R_s (Wang et al., 2023) compared with soils of natural ecosystems. However, the variety of agricultural systems in the Mediterranean is wide (Malek and Verburg, 2017), which can translate into different responses of R_s for crop types and management regimes and therefore it is necessary to study the carbon 50 flows specifically of each agrosystem with its different management regimes.

55 One of the predominant tree crops in the Mediterranean basin is olives (*Olea europaea* L.). Their cultivation has significant economic, social, and environmental consequences for this region, which accounts for more than 90% of global production (FAOSTAT, 2023). Although allowing weed cover in alleys is widely accepted as sustainable crop management (Novara et al., 2021), weed growth is frequently controlled to avoid competition. A drawback of this practice is that the precipitation regime promotes soil erosion in situations where the soil is bare leading to a rise in soil CO₂ emissions (García-Ruiz et al., 2013). In addition, irrigation is a common practice in this crop during water scarcity periods when olive trees typically decrease their photosynthesis and, consequently, their yield during extended drought periods (Moriana et al., 2003). These different management options and inputs influence seasonal soil CO₂ emissions in Mediterranean olive agroecosystems (Montanaro et al., 2023) because they can affect the factors that control R_s . Also root exudates can promote CO₂ emission (Davidson and 60 Janssens, 2006) and create spatial gradients in R_s in the typical olive grove.

Although soil temperature is the main driver of Mediterranean soil CO₂ emissions (González-Ubierna and Lai, 2019), water availability is a limiting factor. Therefore, the typical non-linear growth in R_s as soil temperature increases is modulated by soil moisture in semi-arid areas. Furthermore, the factor by which R_s increases for every 10 °C rise in temperature, known as

the apparent Q_{10} (Davidson and Janssens, 2006) and frequently used to model R_s , is in turn influenced by other different drivers
65 in semi-arid regions. Q_{10} is rarely measured continuously and obtaining this parameter uninterrupted could elucidate the
existence and interdependence of more R_s drivers. Additionally, rain-pulse events play a key role in semi-arid regions (e.g.,
Mediterranean) during dry seasons, and may alter the annual carbon balance. The Birch effect (Birch, 1964) describes how
carbon dioxide emissions increase by a high rate of rapid mineralization after the soil is rewetted due to a rain pulse event. .
This mechanism can contribute to 5% of total annual respiration in semi-arid regions (Delgado-Balbuena et al., 2023), can
70 reduce significantly the annual net carbon gain (Jarvis et al., 2007), and has not been continuously explored in olive grove
soils. Moreover, the expected alterations in precipitation patterns may exert more substantial impacts on R_s than projected
temperature increases (Li et al., 2020). Therefore, water is a critical determinant of R_s , and the techniques used to understand
 R_s drivers in temperate climates (especially focused on temperature) are not applicable in Mediterranean-type climates because
other drivers covary with soil moisture.

75 R_s measurements are usually made at specific times, which makes it difficult to identify the drivers of R_s . In olive groves, R_s
has been studied using impedance measurements (Sierra et al., 2016), the respirometric method (Álvarez et al., 2007; Gómez
et al., 2009), gas chromatography (Marzaioli et al., 2010), process-based modeling (Nieto et al., 2013), or manual chamber
systems (Testi et al., 2008; Almagro et al., 2009; Bertolla et al., 2014; Turrini et al., 2017; Chamizo et al., 2017; Taguas et al.,
2021; Panettieri et al., 2022; Montanaro et al., 2023). The chamber system is widely used; however, in most cases,
80 measurements are performed on favorable weather days during (weekly or monthly) manual diurnal campaigns. Non-
continuous measurements have limitations regarding statistical replication, temporal dependency, annual budgets, and the
related level of uncertainty (Vargas and Le, 2023). It is necessary to generate precise long-term predictions of soil respiration
(R_s) under varying environmental circumstances to enhance our understanding of its impact on R_{eco} (Sánchez-Cañete et al.,
2017). Continuous measurements provide information at all temporal scales and can reveal phenomena that occur at times
85 when sampling is not usually performed, such as at night or during rain events, and can be key to understanding the multitude
of processes influencing R_s . In this sense, the eddy covariance (EC) technique has emerged as a significant tool, enabling the
assessment of ecosystem CO_2 vertical fluxes over extensive spatial and temporal scales, while preserving the integrity of the
studied ecosystem (Reichstein et al., 2005; Baldocchi, 2020). Because most ecosystem respiration (R_{eco}) is due to R_s , it is
common to use the Net Ecosystem Exchange (NEE) values measured with the eddy covariance technique to model R_{eco} as a
90 proxy for R_s . However, the models used are limited because they include aboveground respiration and do not consider the
spatial heterogeneity of R_s as well as the multitude of determinants involved in R_s processes.

Variability in R_s is not only temporal but also spatial (Stoyan et al., 2000), even for a “homogeneous” landscape system such
as a bare-soil olive grove. Although the spatial variability of R_s in olive groves has been somewhat studied (Bertolla et al.,
2014; Montanaro et al., 2023), the difference between R_s under trees versus alleys has not been studied before. In the vicinity
95 of the olive tree, we expected to find higher R_s values because of autotrophic respiration of the roots and an increase in
heterotrophic respiration due to the contribution of photo substrates (Högberg et al., 2001). On the other hand, in the alley, we

expected to find lower R_s because there is negligible autotrophic respiration or photo substrates. Therefore, the main objectives of this study were to i) determine the temporal and spatial variability of R_s in an olive grove ii) analyze the main environmental drivers in R_s and its temporal and spatial dependence, including rain pulse events; and iii) assess modeled ecosystem respiration (100 R_{eco}) using data from an eddy covariance tower comparing it with upscaled ecosystem R_s of the olive grove. To address these objectives, we analyzed a full year's worth of soil and ecosystem respiration in an olive grove in southern Spain measured with an automatic multi-chamber system.

2 Material and Methods

2.1 Site description

105 This study was conducted in an irrigated olive grove (*Olea europaea* L. Arbequina) from Cortijo Guadiana (37°54'45" N; 3°13'40" W; 370 m.a.s.l.), in Úbeda (Jaén, Spain). Castillo de Canena, SL owns this traditional olive grove. The region experiences a Mediterranean climate (Köppen classification: Csa) with dry and warm summers, a mean annual temperature of 16 °C, annual precipitation of 470 ± 160 mm, and potential evapotranspiration of 1205 ± 95 mm (n = 18; IFAPA, 2022). Between March and November, the olive trees received nocturnal drip irrigation three times per week (32 L h⁻¹ for 8 hours). These trees were situated in clay loam soil and were subjected to fertigation, in which each tree received an additional 25–40 g of NPK fertilizer every night. The trees have an approximate height of 4 m, an age of ~85 years, a leaf area index of 1.89 ± 0.17 m² m⁻² and an estimated canopy radius of 2.8 ± 0.3 m. The plantation layout follows a 12x12 m frame, resulting in a tree distribution of approximately 69-70 trees per hectare, with 27% canopy cover (Data obtained with Google Earth and ImageJ software). In 2014, a homogeneous and flat parcel of the olive grove was selected for the application of 110 glyphosate-based herbicide in fall and winter to prevent plant growth. Since then, the soil of the plot has remained bare most of the time and extra herbicide has been applied to prevent rebound of the herbaceous cover and keep maximum control over 115 external conditions. For soil characterization, see Aranda-Barranco et al., (2023).

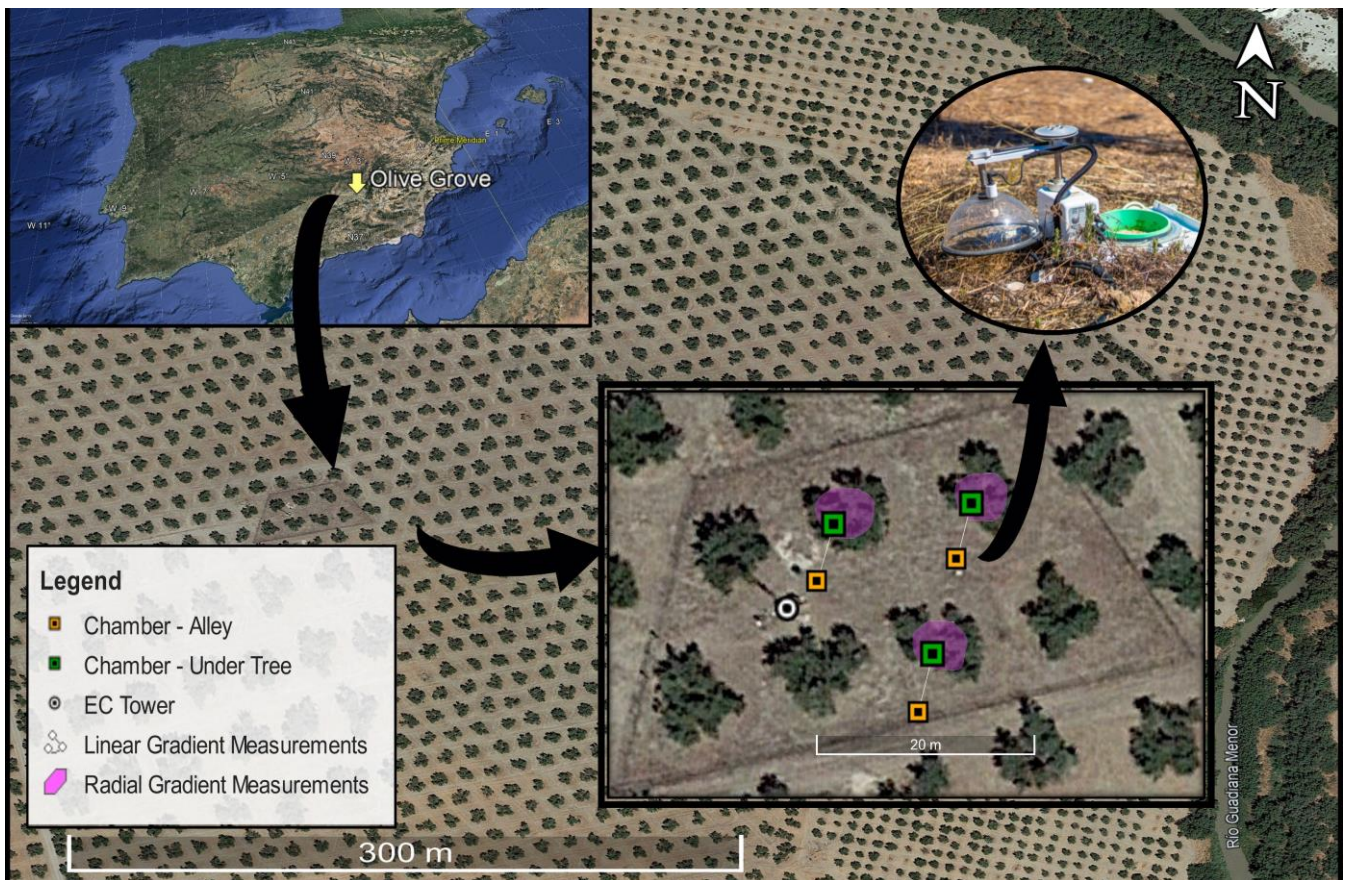
2.2 Soil Respiration

2.2.1 Continuous Measurements

120 In June 2020, six automatic soil CO₂ flux chambers were installed in an olive grove parcel treated with herbicide over PVC collars (20 cm internal diameter) inserted into the soil at similar depths one week before starting the measurement. For volume correction, the average height of each collar was measured (n = 4) at the beginning of the installation. The system was composed of one IRGA (LI-8100A, Li-Cor, Lincoln, NE, USA) coupled to a 16-port multiplexer system (LI-8150, Li-Cor, Lincoln, NE, USA) with 3 opaque chambers (8100-104) and 3 clear chambers (8100-104C), the latter on bare soil. The 125 observation interval was 2 min, and the pre-purge and post-purge time lengths were 30 and 45 s, respectively, for a whole cycle every 20 min. The multi-chamber system was configured to measure every 30 min to temporally match the eddy

covariance and meteorological data. The data were downloaded monthly and processed with SoilFlux 4.2.1 Software to obtain a complete year of continuous measurements (~18000 flux values per chamber) by applying the best fit (lower residuals values) to concentration changes with time (76% exponential fit and 24% linear fit). CO₂ fluxes with a coefficient of determination (R²) lower than 0.995 were discarded. Likewise, although the vegetation on the collars was periodically removed, some CO₂ fluxes were discarded because of plant regrowth in some collars. A forward–backward predictor based on autoregressive moving average modeling (ARMA) in the time domain was used to fill the existing and generated gaps (20% of the total dataset) and thus enable annual integration (see Fig S1 in supplementary material). For the rest of the analysis, only direct measurements were used.

To study spatial variability of R_s, three of these long-term chambers were placed under three different trees (R_s - Under-Tree) at 0.8 m from the center of the olive tree and out of the fertigation drippers, while the other three were placed outside the influence of the olive trees, in the center of the alley, (R_s - Alley) at 5.6 m from the epicenter of each olive tree (Fig. 1). All chambers were installed south of the tree.



140 **Figure 1: Location of the olive grove in Spain, soil chamber distribution, area of campaign measurements, and eddy covariance
141 tower position of the experimental site. © Google Earth 2023**

2.2.2 Discrete Campaigns

To study the spatial R_s , specific campaigns were conducted in two different setups. 1) To study the linear R_s gradient between the tree and alley chambers, 15 additional collars were installed between long-term chambers (5 collars for each tree-alley

145 location) to accommodate manual measurement campaigns. A portable IRGA (Li-7810 attached to a Smart Chamber, Li-Cor, Lincoln, NE, USA) was used to quantify R_s manually through 8 campaigns between September and December 2021. 2) To study the angular R_s gradient, 48 collars were installed surrounding the 3 selected trees (16 collars for each tree) and 9 campaigns were conducted during 2022 to quantify variations in R_s concerning the orientation. To project R_s to the ecosystem

150 scale ($R_{s,eco}$), we weighted the alley and the under-tree R_s , first as a function of the ground and canopy cover, second as the average R_s value of the alley and the under-tree linear gradient, and third as a correction for measuring in the south facing direction (Table 1). For estimation of canopy coverage, an average of 50 canopy areas were measured using Google Earth

snapshot and imageJ Software. To know the part of the linear gradient that belongs to the tree and alley another 50 canopy

lengths (each one as the average of four cardinal measures) were measured and averaged. The results shown in Fig 10 (arrows)

were used to know the average value of the 'Under-Tree' and 'Alley' linear gradient. Simultaneous measurements of Li-7810

155 and Li-8100 showed a slope of 0.78 with $R^2 = 0.95$. The differences in magnitudes between the two instruments could be due

to a the time lag of between 5 and 30 minutes in that comparison or due to the two different optical techniques. Such

discrepancies are found even between same IRGAs model (Kutikoff et al., 2021). Nevertheless, only relative values

alley/UnderTree of 7810 campaigns were used in this study.

*Table 1 Correction and weighting coefficients for the homogeneous
calculation of $R_{s,eco}$ (See Fig 8)*

	<i>Weighting by Canopy/Alley Coverage (%)</i>	<i>Longitudinal correction factor</i>	<i>Orientation correction factor</i>
Alley	73	1.2	NA
Under-Tree	27	0.7	0.9

160 2.3 Ecosystem Respiration.

Throughout the study duration, ecosystem respiration (R_{eco}) was estimated from Net Ecosystem Exchange (NEE) measurements made within the olive grove employing the Eddy Covariance (EC) technique. An EC tower was set up in the center of the agroecosystem, with instruments positioned at a height of 9.3 m (5.3 m above the canopy). These instruments were used to monitor CO_2 levels and wind speeds at 10 Hz. Gas densities were measured using an enclosed-path infrared gas 165 analyzer (IRGA, Li-Cor 7200; Lincoln, NE, USA). Simultaneously, wind speeds in the three vector components were recorded using a sonic anemometer (CSAT-3, Campbell Scientific, Logan, UT, USA).

EddyPro software version 7.0.8 computed the half-hourly NEE. Anomalies such as spikes, trends, dropouts, and abrupt variations in the eddy covariance data were filtered using the methodology outlined by Vickers and Mahrt (1997). Time lags between gas concentrations and wind speeds were compensated using covariance maximization. Half-hourly values of means, 170 variances, and covariances were computed using the Reynolds decomposition rules. Double rotation of coordinates and spectral corrections for high frequency (Fratini et al., 2012) and low frequency (Moncrieff et al., 2006) were applied. Finally, the resulting fluxes were filtered according to the quality control method proposed by Mauder et al. (2013), and additional filters were applied to the half-hourly fluxes using the methodology described by (Chamizo et al., 2017).

Approximately 48% of the data gaps in the agroecosystem measurements were attributed to missing data in the eddy covariance 175 system, primarily stemming from adverse meteorological conditions, night-time stability conditions, instrumentation malfunctions, or quality control filters. We employed empirical modeling to fill in the missing data. Within the continuous eddy covariance database, we used the marginal distribution sampling technique (Reichstein et al., 2005) to replace missing values. This method is based on the replacement of missing values using a time window of several adjacent days. After 180 replacing missing data, we applied two semi-empirical models to partition NEE into two components: gross primary production (GPP_{eco}) and ecosystem respiration (R_{eco}). The Reichstein et al. (2005) model R_{eco - NT} is night-time based and it extends an exponential function of daytime respiration based on night-time data (with the assumption that GPP_{eco} is negligible during night-time periods) to estimate daytime periods. The Lasslop et al. (2010) model estimates respiration (R_{eco - DT}) from fitting the Light-Response Curve during the daytime. Missing data replacement and partitioning were performed using the REddyPro R Package (Wutzler et al., 2018).

185 2.4 Environmental Measurements

Soil temperature (T_s) and soil water content (SWC) were measured at a depth of 5 cm near each chamber using a 190 thermistor (LI- 8150-203, Li-Cor, Lincoln, NE, USA) and ECH2O model EC-5 soil moisture probes (Decagon Devices, Inc., Pullman, WA, USA). In addition, complementary environmental measurements were performed at the experimental site. The air temperature and relative humidity were recorded using a thermohygrometer (HC2S3, Rotronic, AG, Bassersdorf, Switzerland) positioned at a height of 5 m. The vapor pressure deficit (VPD) was computed using the data provided by the 195 thermohygrometer. Incoming and outgoing components of short-wave and long-wave radiation were monitored using a four-component radiometer (CNR-4, Kipp and Zonen, Delft, Netherlands) positioned at a height of 7 m and situated 2 m away from the tower. This setup allowed the determination of the net radiation and albedo. Incident and reflected PAR were also measured at 7 m using photodiodes (quantum sensor; Li-190, Lincoln, NE, USA). These meteorological data were sampled at 30-s intervals, averaged over 30-min periods, and subsequently stored in a data logger (CR3000, CSI).

2.5 Rain Pulse Events

The days between precipitation (PPT) events were counted to identify rain pulses. Intervals between PPT events (hereafter inter-event periods, IEPs) were counted in days from the last PPT event, with a magnitude higher than 0.4 mm. The daily timescale was selected to avoid confounding diurnal R_s variability and to achieve robust analyses. Once the event is reached, if there is rain on the following day, the IEP is reset to 1. The R_s one day before the PPT event was taken as a reference. The R_s event-response effect (ΔR_s) was measured as the difference between the mean daytime R_s post-event and the mean daytime R_s pre-event.

The increase in the soil water content (ΔSWC) was calculated analogously as in Equation 1. A rain pulse event was considered when the value of the difference of R_s concerning the previous day was > 2.5 medians of the entire R_s time series and coincided with a precipitation event. A potential fit was performed with the data excluding those whose value of the residual exceeds $3 \mu\text{mol CO}_2 \text{ m}^{-2} \text{ s}^{-1}$.

2.6 Q_{10} calculations

Weekly windows were used to calculate Q_{10} . For this, an exponential adjustment was conducted according to

$$R_s = ae^{bT_s}, \quad (2)$$

To then calculate Q_{10} as

$$Q_{10} = e^{10b}, \quad (3)$$

210 Where 'T_s' is soil temperature (°C), 'a' represents the R_s intercept at a soil temperature of 0°, and 'b' serves as the temperature coefficient, indicating the temperature sensitivity of R_s and playing a role in the calculation of Q_{10} (Lloyd and Taylor, 1994).

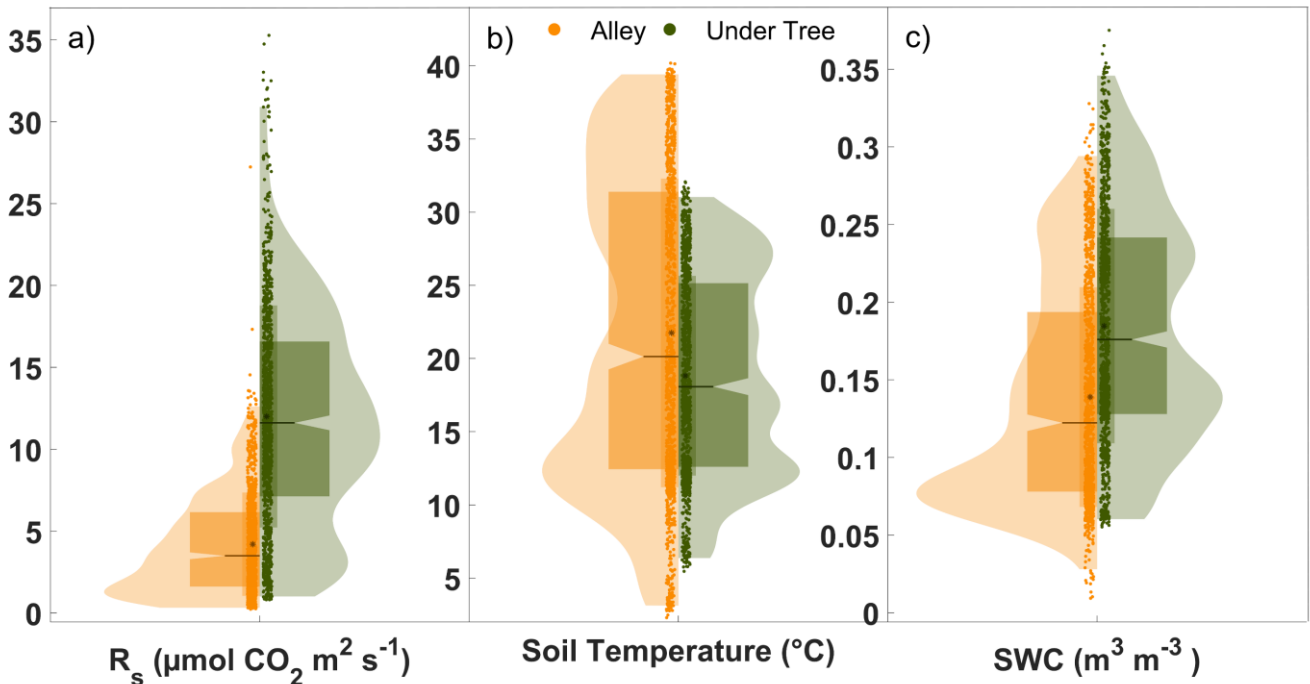
2.7 Statistical Analysis

We used 30-min values to characterize the diurnal variations, Q_{10} , and spatial gradients of R_s . Data at daily scales were used for the rest of the analysis, including a description of rainfall pulses, seasonal variability, and establishment of 215 significant differences between trees and alleys. Polynomial curve fitting was used to optimize the relationship between ΔSWC variations as a function of the independent variables of precipitation and the previous SWC. The Shapiro-Wilk test determined the non-normality of the variables. The probability distribution of the variables was evaluated using the kernel density. Box plots and nonparametric statistical tests of two independent samples (Mann-Whitney test) were performed on the principal subsets of soil respiration, soil temperature, soil water content, and Q_{10} to identify significant differences in the averages (3 220 chambers) of these variables. The annual balances were calculated as the sum of the daily values and the error was twice the square root of the accumulated variance of the standard deviation of the data. The graphs and statistical analyses were performed using Matlab (version R2020a).

3 Results

3.1 Seasonal variability in R_s and environmental conditions

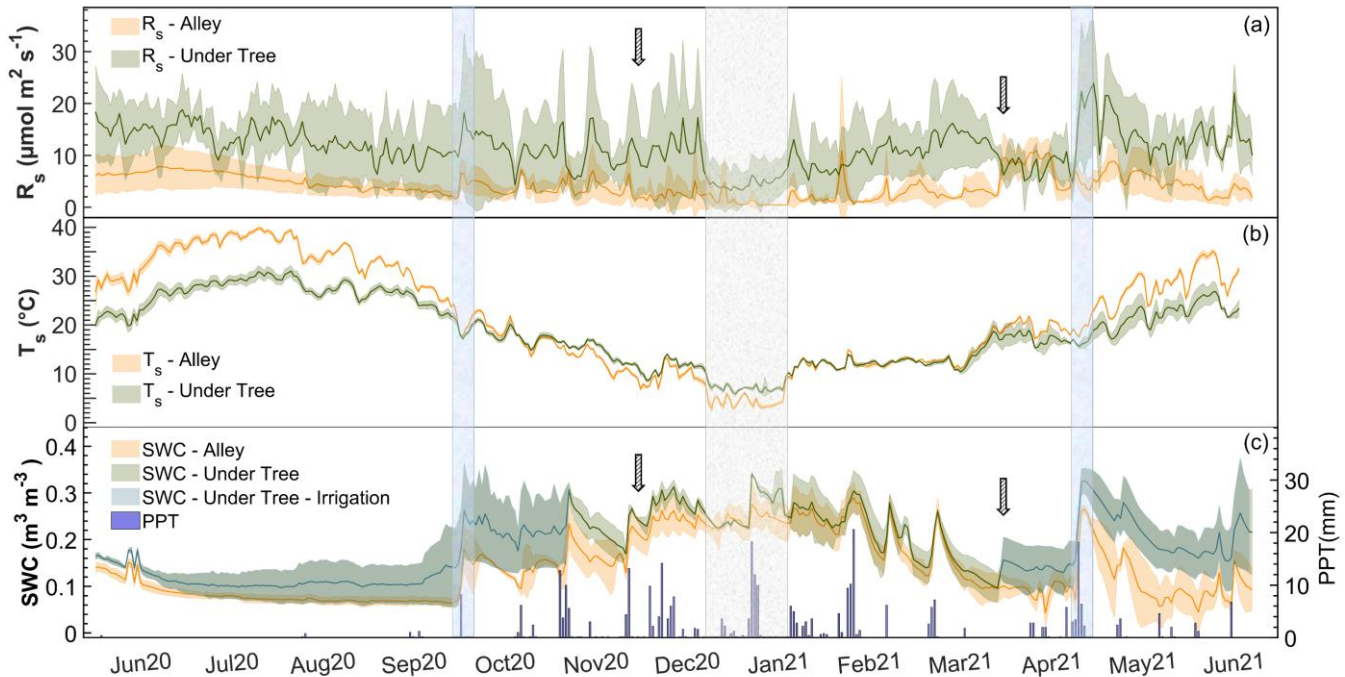
225 Significant differences were found between soil respiration (R_s) under trees and in alleys. Throughout the measurement year, R_s - Under Tree was $11.5 \pm 3.8 \mu\text{mol CO}_2 \text{ m}^{-2} \text{ s}^{-1}$ while R_s - Alley was $4.3 \pm 2.3 \mu\text{mol CO}_2 \text{ m}^{-2} \text{ s}^{-1}$, which means 2.7 times (Mann Whitney test; $p < 0.001$; $n = 17500$) more R_s under the tree (Fig. 2a) than in the alley. The kernel density shows that the highest frequency of R_s - Alley was found around $1.5 \mu\text{mol CO}_2 \text{ m}^{-2} \text{ s}^{-1}$ (due to the low winter values), whereas for R_s - Under Tree, it was close to that of the median ($11.0 \mu\text{mol CO}_2 \text{ m}^{-2} \text{ s}^{-1}$).



230 **Figure 2:** Violin plots showing the daily averages of (a) soil respiration, (b) soil temperature, and (c) soil water content. Orange and green refer to “alley” and “Under-Tree” measurements, respectively, each representing the average of three chambers. The horizontal lines (at the notch) indicate the median and the black dots represent the mean. The curve area is the kernel density, and the wide box represents the range q1–q3.

235 Great seasonal variability in R_s was observed. For both locations R_s increased in the warmer months and decreased in the colder months (Fig. 3a), showing quite different values between months. Daily average minimums of R_s Alley = $0.4 \mu\text{mol CO}_2 \text{ m}^{-2} \text{ s}^{-1}$ and R_s Under Tree = $3.2 \mu\text{mol CO}_2 \text{ m}^{-2} \text{ s}^{-1}$ were reached in January for both spatial locations. In contrast, the maximum R_s - Alley occurred in April ($11.0 \mu\text{mol CO}_2 \text{ m}^{-2} \text{ s}^{-1}$) while the maximum R_s - UnderTree occurred in May ($23.9 \mu\text{mol CO}_2 \text{ m}^{-2} \text{ s}^{-1}$). The R_s of both spatial locations were only similar in April, coinciding with herbicide application. In general, there was greater 240 variability in the R_s data under the tree ($\pm 3.8 \mu\text{mol CO}_2 \text{ m}^{-2} \text{ s}^{-1}$; SD of data at 30 min) than in the alleys ($\pm 2.3 \mu\text{mol CO}_2 \text{ m}^{-2}$

s^{-1} ; SD of data at 30 min), which is visible in the entire daily time series (Fig. 3a). The ratio of R_s -Under Tree to R_s -Alley varied throughout the year. In the coldest months, although respiration decreased in both locations, it was more noticeable in the alley so that magnitudes were reached under the tree of up to 7 times more than in the alleys (see Fig. S3 of supplementary material) when the values of SWC in both locations were equal.



245

Figure 3: Seasonal variation in daily averages under the tree and in the alley of a) soil respiration (R_s), b) soil temperature (T_s), and c) soil water content (SWC) and cumulative daily precipitation (PPT). Solid lines represent the mean of the three chambers, and the shaded area is the standard deviation. The first arrow indicates olive harvest, and the second arrow indicates herbicide application. The blue rectangles indicate two important rain pulses, whereas the gray rectangle indicates the period of the lowest values of R_s and T_s .

250

Differences were observed between soil temperature (T_s) and soil water content (SWC) under trees and in alleys (Fig. 2b,c). During the year of measurement, the average daily values of T_s - Under Tree = 18.8 ± 6.8 °C; T_s - Alley = 21.7 ± 10.5 °C, $SWC_{UnderTree} = 0.185 \pm 0.08$ m³ m⁻³ and $SWC_{Alley} = 0.139 \pm 0.07$ m³ m⁻³ so that T_s - Under Tree was 13% lower (Mann Whitney test; $p < 0.001$; $n = 17500$) than T_s - Alley and $SWC_{UnderTree}$ was 33% higher (Mann Whitney test; $p < 0.001$; $n = 17500$). However, T_s and SWC showed large seasonal variation in the olive grove (Fig. 3b and Fig. 3c). In such a way, T_s - Under Tree was higher than T_s - Alley in the coldest months, showing a buffer effect of the trees on T_s . In general, T_s was more variable in the alleys. More pronounced seasonal variability was observed in the alleys than under the tree, with T_s maximum in July at 31.1 °C under the tree and 39.8 °C in the alleys, whereas minimum T_s was 5.9°C under the tree and 2.8°C in the alley (January). Temperature

variability of the soil was damped in the proximity of the olive tree so that the temperature was higher than that of the alley in
260 the cold months and vice versa. From June to September, the high average daily T_s coincided with the absence of precipitation. The end of the summer (September) presented the lowest daily SWC values of $SWC_{Under\ Tree} = 0.10\ m^3\ m^{-3}$ and $SWC_{Alley} = 0.04\ m^3\ m^{-3}$. (Fig. 3b). The first rainfall raised the SWC until it reached a maximum of $SWC_{Under\ Tree} = 0.34\ m^3\ m^{-3}$ and $SWC_{Alley} = 0.29\ m^3\ m^{-3}$ so that they became equal later (December) after one month without irrigation. The return of irrigation in March again causes a difference in the SWC, which is maintained for the rest of the time series. The annual precipitation was 322
265 mm falling mostly in autumn, winter, and spring (Fig. 3c), when 71 rain episodes were quantified with up to 27% of events with more than 4 mm day⁻¹, and a maximum of 21 mm day⁻¹. 48% of the events occurred on successive days (IEP = 1) and accounted for 53% of the accumulated PPT (Fig. S2a).

3.2 Diurnal and spatial variability in R_s chambers

Spatial variation in R_s among six chambers and the three tree/alley chamber pairs is shown by the inter-chamber variability in
270 Figure 4. In the alleys, we found daily variability with maximum R_s at midday, coinciding with maximum temperatures (Fig. 4). However, the typical daily R_s/T_s bell pattern was not always detected in the three chambers. During July, one alley chamber consistently showed no diurnal variability. In general, in winter, diurnal variability was detected with up to 3 $\mu\text{mol CO}_2\ m^{-2}\ s^{-1}$ more at midday than at night (data not shown). In spring, R_s was between 5 and 9 $\mu\text{mol CO}_2\ m^{-2}\ s^{-1}$ higher at midday versus night (Fig 4. d-f). On the other hand, the high variability of the fluxes under the trees caused the daily trend in R_s to be
275 statistically insignificant ($p_{value} = 0.57$; $n = 240$). However, we find an exception in the hottest summer months when soil respiration decreases in the afternoon while VPD increases. ($p_{value} < 0.05$; $n = 240$; Fig 5, a-c).

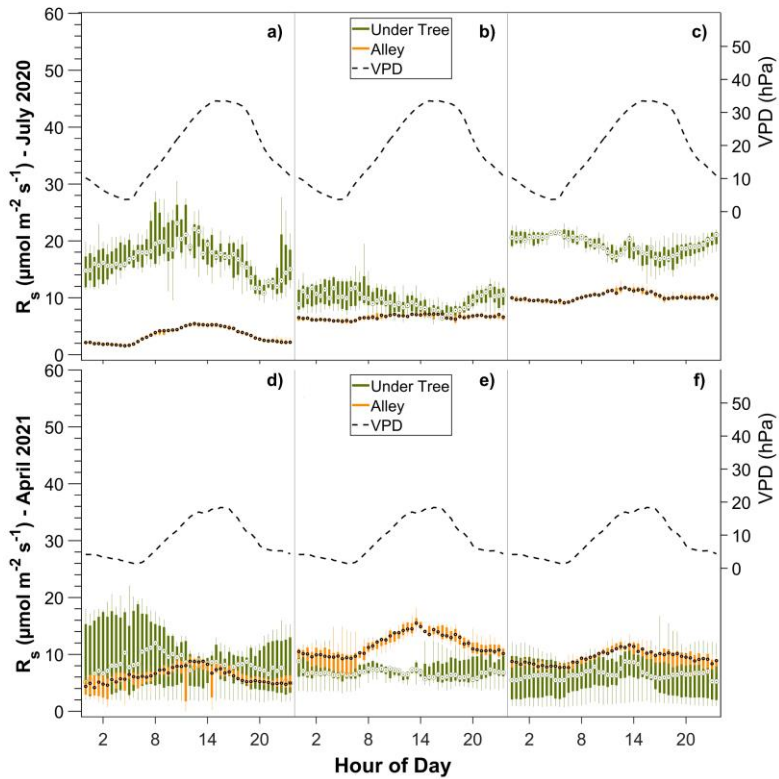


Figure 4: Daily variability of Rs in the three pairs of alley/Under-Tree chambers in one week of data in July (a,b,c) and one week of data in April (d,e,f). The bars represent box plots of 30-min data during the week.

280 Moreover, we found marked spatial variability in Rs both under the canopy and in the alley. In the alleys, sometimes up to 3 times more respiration is observed in one chamber compared to another (Fig. 4; compare panels a and c), but these differences between chambers, in turn, vary over time in such a way that a given chamber can sometimes measure the greatest and sometimes the least CO₂ emissions (switch in magnitude of chambers 2 and 3 between July and April; Fig 4; compare panels b/c and e/f).

285 **3.3 Q₁₀ variability**

Seasonal variability was found in weekly Q₁₀ values, especially under the tree (Fig 5). In the alley, Q₁₀ ranged between 1.2 (warm months) and 2.0 (cold months), whereas under the tree, Q₁₀ ranged between 0.6 (warm months) and 1.8 (cold months). In general, the Q₁₀ Under-Tree was lower and more variable than in the alley. Values for the entire study period were Q₁₀ Alley = 1.69 ± 0.40 and Q₁₀ Under Tree = 1.10 ± 0.66 (Mann Whitney test; p < 0.01). Hysteresis behavior was identified for R_s Alley in 290 summer data when plotted with both T_s and SWC. A linear relationship was found between the Q₁₀ and the SWC and soil temperature under the tree (Q₁₀ = 1.120 - 0.026T_s + 2.292SWC; R² = 0.36) such that as the temperature increased and the SWC decreased, Q₁₀ < 1 values were obtained. This relationship was not observed in the alleys.

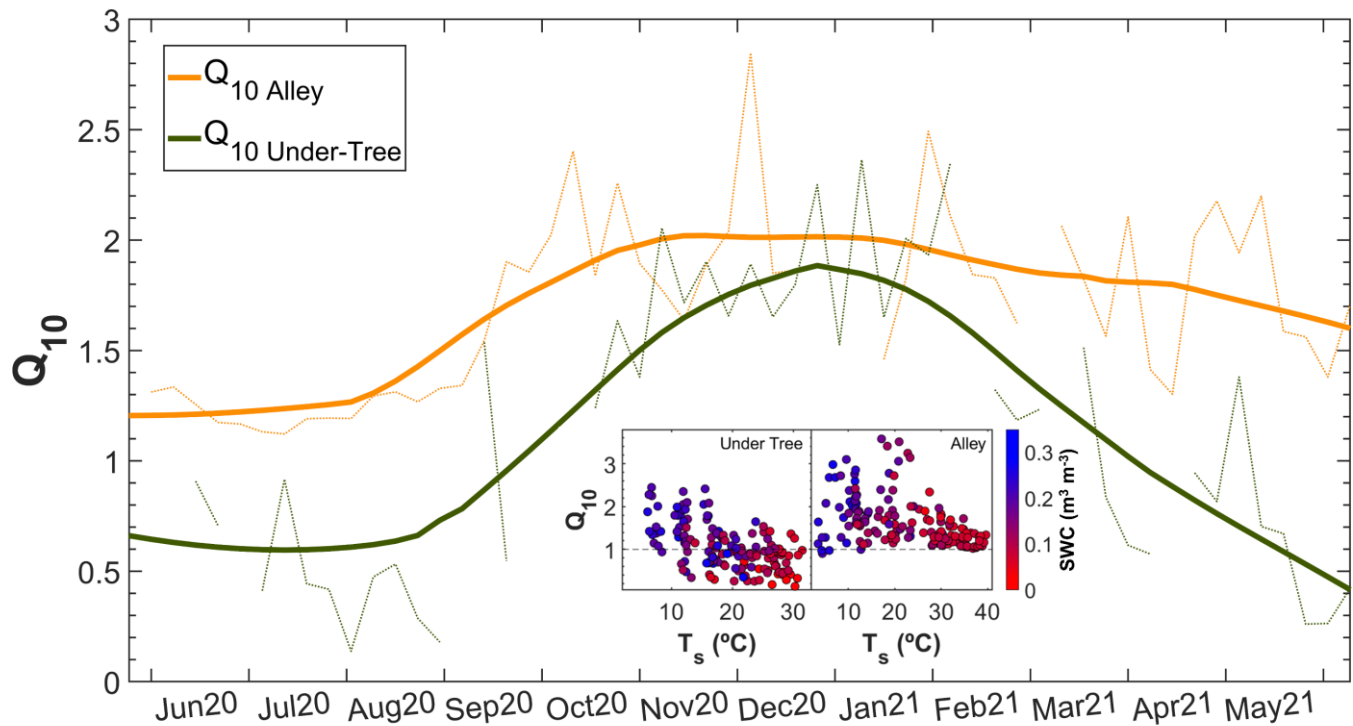


Figure 5: Seasonal variation in Q_{10} parameter in the alley and under-tree chambers. Dashed lines are the weekly Q_{10} values, and

295 **solid lines refer to the moving average daily values (± 14 adjacent day window). The inner figure shows the relationship of weekly**

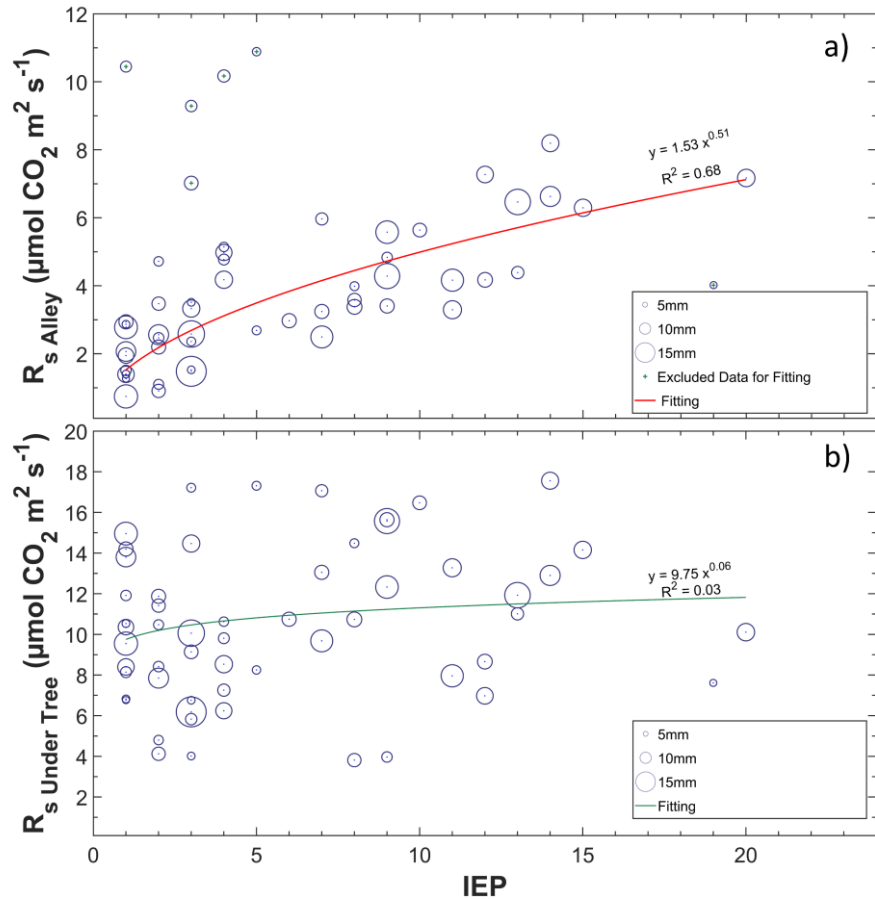
Q_{10} to weekly average soil temperature and soil water content (SWC) for the two locations.

3.4 Rain Pulses events: R_s and R_{eco}

Of the seventy-five precipitation events, forty-one were accompanied by enhanced R_s . This was especially frequent when rain fell on dry soil, and the increased R_s rates followed the longest inter-event periods (IEPs), as shown in Figure 6a. 300 The PPT size does not have much influence on ΔR_s (data not shown). However, the four highest magnitude R_s values were found in the lowest IEP and PPT in the alleys but were excluded from the regression as they were statistically classified as anomalies. In this way, notable rain pulses were detected when the IEP was large and $SWC < 15\%$ (Fig. 7a), whereas rainfall pulses were scarce in months when the soil contained a moderate amount of water ($> 15\%$). The relationship between R_s and PPT was lost with SWC values higher than 15% in alleys and 20% under trees (Fig. 7b and Fig. 7c). The increase in R_s with 305 the appearance of a PPT event followed a nearly linear relationship in the alleys when $SWC < 15\%$ ($p_{value} < 0.01$; $r = 0.902$), whereas, under the tree, the increase was when $SWC < 20\%$ and less intense ($p_{value} = 0.06$; $r = 0.456$). The R_{eco} (ecosystem

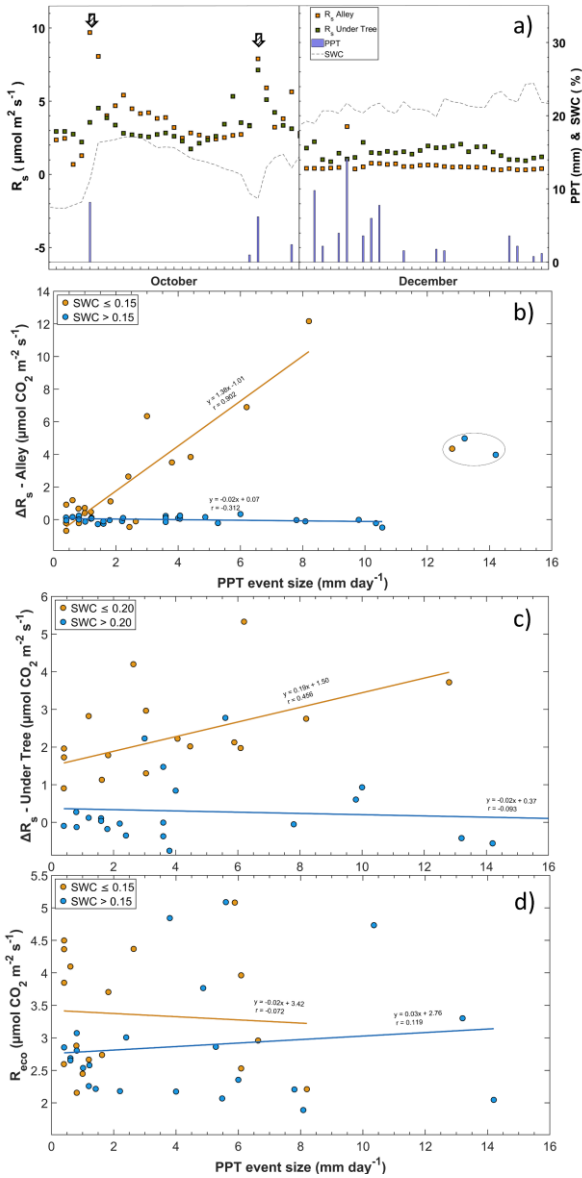
respiration) values obtained via modeling appear not to respond to rainfall pulses (Fig. 7d), whether the soil was previously

dry ($p_{value} = 0.78$; $r = -0.072$) or not ($p_{value} = 0.59$; $r = 0.119$). The rain pulse events implied an annual accumulated flux of 310 g C m⁻² in the alleys and 110 g C m⁻² under the tree.



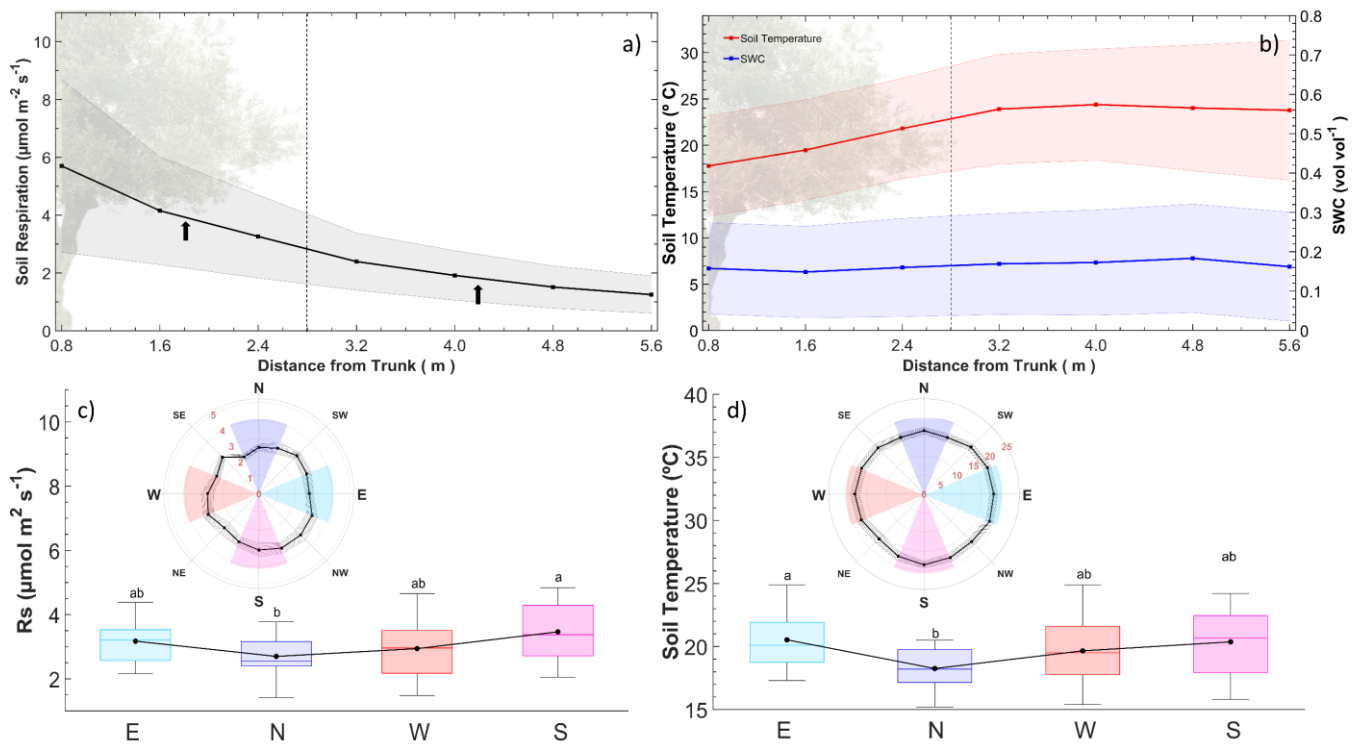
310

Figure 6: Relationship between inter-event period (IEP) and daily soil respiration (Rs) in alleys (a) and Under-tree (b). The different sizes refer to the relative magnitude of the precipitation event, with the minimum being 0.4 mm and the maximum being 21 mm (daily values).



315 **Figure 7: Relationship between rainfall and soil respiration (R_s).** a) Rain pulses in a period with low soil water content (SWC) at the onset of the rain event (a; left) and a period with moderate SWC (a; right). Arrows indicate the moment of the pulse b) the relationship between the size of the PPT event (mm day^{-1}) and the variation in soil respiration rate (ΔR_s ; $\mu\text{mol CO}_2 \text{m}^{-2} \text{s}^{-1}$) in the alley and c) under the tree. Measurements inside the circle are outside the fit. d) Relationship between the size of the PPT event (mm day^{-1}) and ecosystem respiration (R_{eco} ; $\mu\text{mol CO}_2 \text{m}^{-2} \text{s}^{-1}$). The lines represent linear regressions, and r is the correlation coefficient.

Manual measurement campaigns revealed exponential transitions in both R_s and T_s in linear gradients from the tree to the alley (Fig. 8a and Fig. 8b). From 3.2 m away (4th collar from the tree), significant differences in R_s and T_s (Mann-Whitney test; $p < 0.05$) were found relative to the chamber closest to the tree. However, from 3.2 m outwards, T_s stabilized, while R_s continued to decrease slightly. Because the average distance under the canopy from the epicenter of the trees was 2.8 ± 0.3 m, we can differentiate these two independent areas in terms of different R_s behaviors. Thus, to project the value of R_s to the ecosystem scale, two areas were considered where the average value used to weigh was the midpoint of the interpolation between sampled points (arrows in Fig. 8a). Regarding angular gradients, R_s was higher on the south side than on the north side ($n = 27$; $p < 0.05$) during the sampling campaigns (Fig. 8c), and the temperature was higher on the east side (Fig. 8d) than on the north side ($n = 27$; $p < 0.05$). The high variability in SWC was driven by punctual irrigation and prevented detection of significant differences in soil water content. Because the chamber was installed in the south, it was weighted according to these differences to scale up R_s (Supplementary material).



335 **Figure 8: Longitudinal and angular gradients of soil respiration (R_s), soil temperature (T_s), and soil water content (SWC). (a) R_s measurements in a linear gradient from tree to alley collars. Each point represents the average (\pm standard deviation) of the manual measurement collar, and the line is a linear interpolation. The dashed vertical line refers to the separation between the 'Under-Tree'**

and 'Alley' regions of the transect (black arrows). The midpoint of the gradient of each region is considered as the weighting factor for R_s . (b) T_s and SWC variations in a linear gradient from the tree to alley collars ($n_{collar} = 8$); (c–d) Angular gradient of R_s and T_s and differences between orientations. Each point represents a manual measurement collar, and the line represents a linear interpolation. Areas in the angular graphic represent the cardinal grouping of the three measurements, and the box plot refers to 340 the 9 campaigns ($n = 27$).

3.6. Upscaled $R_{s,eco}$ vs. modeled R_{eco} .

The response of net ecosystem exchange (NEE), soil respiration upscale to ecosystem level ($R_{s, eco}$), and ecosystem respiration (R_{eco}) to various rainfall pulses is represented in Figure 9 and we can observe that they respond in separate ways. The occurrence of a PPT event in September implied an increase in $5 \mu\text{mol CO}_2 \text{ m}^{-2} \text{ s}^{-1}$ of $R_{s,eco}$ and $3 \mu\text{mol CO}_2 \text{ m}^{-2} \text{ s}^{-1}$ of 345 NEE, whereas R_{eco} did not respond (Fig. 9). Similar patterns occurred in the other rainfall events in November and June. These increases in $R_{s,eco}$ that were not reflected in R_{eco} may indicate an underestimation of respiration balances, as well as errors in GPP_{eco}. Regardless of rainfall, R_{eco} was underestimated concerning $R_{s,eco}$ in the warm months, whereas in the cold months, the magnitudes of both approaches were similar (Fig. 10b and Fig. 10c). On average, R_s Under-Tree represented 39% of $R_{s,eco}$ although the fraction was variable, with maximal contributions of 55% (winter) and minimal contributions of 25% (Fig. 10a). The soil 350 surface classified as "under trees" represents 27% of the olive grove, which indicates that in winter half of the soil respiration of the olive grove originates in a soil that covers a quarter of the total surface of the land.

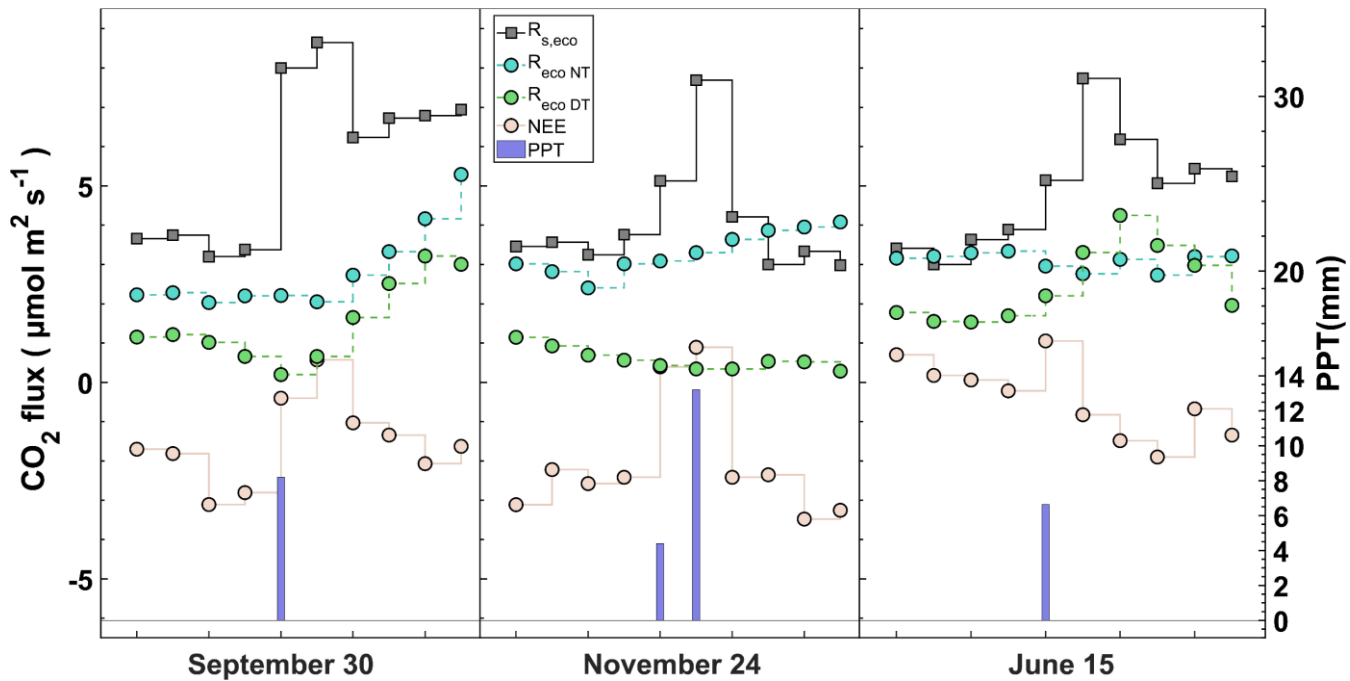
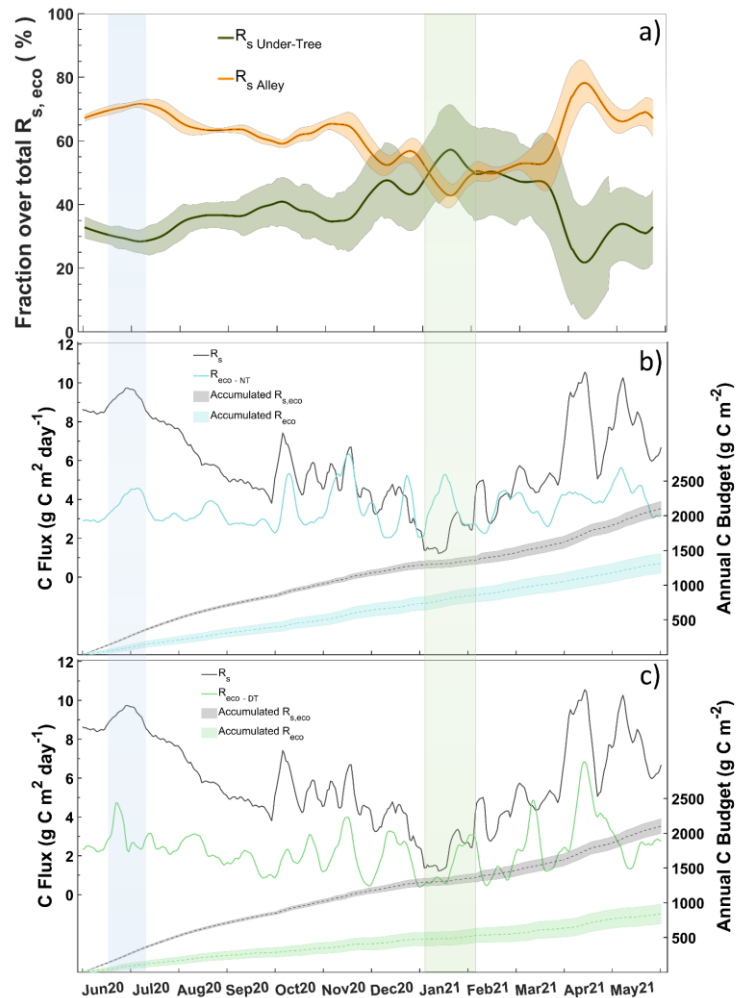


Figure 9: Response of CO₂ fluxes (daily average) to a precipitation event at three different times in the time series. Net ecosystem exchange (NEE), soil respiration upscaled to the ecosystem level ($R_{s, eco}$), night-time modeled ecosystem respiration ($R_{eco - NT}$) and

355

day-time modeled ecosystem respiration ($R_{eco - DT}$).

We show two approaches with the annually integrated R_{eco} as the combination of measurement and empirical modeling based on EC data ($R_{eco-NT} = 1310 \pm 160 \text{ g C m}^{-2}$; $R_{eco-DT} = 850 \pm 140 \text{ g C m}^{-2}$) and upscaling through chamber data ($R_{s, eco} = 2100 \pm 50 \text{ g C m}^{-2}$). During the warm months, the magnitudes of the chamber and night-time EC approaches are quite different, although they are consistent in the temporal variation. However, although the magnitudes are closer during the cold 360 months, there is an inverse relationship between the two approaches. The daytime approach neither covaries with nor has similar magnitudes to respiration data from chambers in hot months. On the contrary, the response of $R_{eco - DT}$ is more like chambers the higher the influence of $R_{s, Under-Tree}$ on the ecosystem (Fig. 10a and Fig. 10c).



365 **Figure 10: a) Fraction of daily R_s Alley and R_s Under-Tree overestimated $R_{s,eco}$. b) Daily values of $R_{s,eco}$ and R_{eco-NT} during the year (left) and the cumulative value of both (right). C) Daily values of $R_{s,eco}$ and R_{eco-DT} during the year (left) and the cumulative value of both (right). The blue rectangle marks the warm period and high R_s alley influence. The green rectangle is the cold period and high R_s Under Tree influence.**

4. Discussion

370 This study relies on a dataset spanning one continuous and complete year of respiration fluxes at soil and ecosystem scales and provides significant insights into the temporal and spatial variations of olive grove respiration as well as influencing factors. The abundance and continuity of half-hour measurements under trees and in alleys allow us to describe processes and trends that have not been described in olive groves by typical studies based on manual campaigns.

4.1 Spatial differences

375 Our findings affirmed a clear seasonal variability of R_s and its main drivers (SWC, T_s), which is reflected in a high range of values compared with other studies using chambers. Bertolla et al. (2014) and Testi et al. (2008) measured daily values between $1.3 - 8.8 \mu\text{mol m}^2 \text{s}^{-1}$ ($n = 16$) and $2.3 - 5.9 \mu\text{mol m}^2 \text{s}^{-1}$ ($n = 5$; monthly) near the trunk of irrigated olive trees, whereas our study showed a wider range of $3.2 - 23.9 \mu\text{mol m}^2 \text{s}^{-1}$ ($n = 365$; daily). Such differences could be explained by the difference in the tree age (85 years for our individuals, versus primarily juvenile individuals between 2 and 7 years) which mean bigger and larger root systems. Juveniles will have less root development whose autotrophic and heterotrophic respiration 380 is expected to be lower than that of an adult individual. In our study, we can deduce a predominant influence of respiration associated with the roots on the total soil activity, since R_s was increasing as the measurements approached the trunk and $R_{s-UnderTree}$ exceeded on average three times that observed in the alleys on average. This excess changed during the year, being between 2 and 15 times higher during the warmest and the coldest months, respectively (Fig. S3a). Since the soil water content 385 was similar in the cold period (Fig. S3c), the big differences could be due to i) heterotrophic respiration decreases in the alleys due to the additive effect of a higher Q_{10} (Fig. 5) and a higher decrease in the temperature versus under the canopy (Fig. S3b); and ii) higher heterotrophic $R_{s-UnderTree}$ due to a higher temperature compared to the alleys and differences in the substrate due to the addition of root exudates and superficial leaf litter (Davidson and Janssens, 2006) meaning higher soil organic carbon under the tree canopy. The contribution of heterotrophic respiration to total respiration is complex to estimate (Comeau et al., 390 2018) and these data are not available. Nevertheless, considering that the magnitude of $R_{s-Alley}$ during the winter was very small, we assumed that the contribution of heterotrophic respiration under the tree is also small; therefore, the $R_{s-UnderTree}$ was largely controlled by rhizosphere respiration (R_z), which is the sum of heterotrophic respiration linked to the root system and autotrophic respiration for maintenance and growth of the roots.

395 Continuous measurements allowed us to study the contribution of each location to the total R_s . Despite the total canopy fraction “Under Tree” being only 27% in our agroecosystem, there are periods where the proportion of $R_{s-UnderTree}$ contributes more than 50% to the $R_{s,eco}$ (Fig. 10a). Therefore, it cannot be assumed that the R_s Alleys are representative of olive groves and most

likely of mosaic tree crops such as savannas or ‘dehesas’. In fact, in other systems with an open area/canopy distribution (Tang et al., 2005), R_s Under-Tree was an order of magnitude greater than R_s - Alley; however, because the spatial gradients of R_s were not quantified, the estimate at the ecosystem scale is unknown. In this study, we quantified the gradient between the measurements taken under the tree and in the alleys and found an exponential decrease as we moved away from the trunk that allowed us to 400 do a simple upscaling. Although the influence of the roots extends gradually throughout the crop, its effect on respiration appears to be reduced significantly around a 3-m separation. Therefore, for this experimental site, the canopy radius (2.8m on average) can be a good proxy for determining the significant separation between the under-tree rooting zone and alley. Other 405 studies have established a random collar sampling map (for instance see Turrini et al., 2017) with different separation distances around the olive tree, which makes it difficult to integrate the role of rhizosphere respiration if longitudinal correction factors are not applied (Table 1). Moreover, we found more respiration on the south side of the trees, where the temperature was also higher. Although the campaigns in which the gradient data were taken, only covered 4 of the 12 months of the year, and spatial 410 differences may also vary over time, we have used the data obtained to weigh and scale the values of R_s at the ecosystem scale and thus estimate $R_{s,eco}$.

4.2 Eddy covariance models comparison

410 The use of automatic chambers made it possible to assess annual balances of R_s . In the estimation of model R_{eco} with data derived from EC, we obtain an annual balance of 850 gC m^{-2} (Daytime approach) and 1300 gC m^{-2} (Nighttime approach), whereas if we project R_s at the ecosystem scale ($R_{s,eco}$), we obtain 2100 g C m^{-2} (Fig. 12 b). The values obtained here with 415 chambers may be similar to those found in grassland meadows (1990 g C m^{-2} ; Bahn et al., 2008) and higher than other previous estimations in olive groves ($860 \pm 150 \text{ g C m}^{-2}$) although they were measured in monthly or bimonthly campaigns (Jian et al., 2021). A priori, $R_{s,eco}$ should be less than R_{eco} because $R_{s,eco}$ is a fraction of R_{eco} ($R_{eco} = R_{s,eco} + R_{AboveGround}$). However, the 420 accumulated values obtained from the chamber ($R_{s,eco}$) are higher those obtained from the EC (R_{eco}), especially in summer. The chamber method takes snapshots of R_s , whereas the partitioning NEE method use a seven-day sliding window for their calculations. Furthermore, errors may be made in the NEE partitioning method, such as the underestimation of nocturnal fluxes due to low turbulence or the erroneous assumption that nocturnal respiration can be perfectly extrapolated to daytime 425 respiration. On the other hand, during the day, we observe inverse relationships of R_s - Under Tree/ T_s to those that models based on NEE partitioning usually assume (Q_{10} values < 1 in Fig. 5) and that could lead to an erroneous estimate of R_{eco} by the daytime method. Moreover, the greater the role of above-ground tree respiration on R_{eco} , the worse the relationship between the $R_{s,eco}$ and R_{eco-NT} (Fig. 10a and Fig. 10b), which indicates that the widely accepted partitioning model based on Reichstein et al. (2005) does not apply correctly to this semi-arid ecosystem. It is expected that Lasslop et al., (2010) would have greater 430 agreement when the influence of the R_s Under Tree is greater (Fig. 10) since R_{eco} calculates it from the photosynthetic organisms' activity. Since each model is based on different mechanisms, we can say that no method faithfully represents the ecosystem, and furthermore there are more drivers than temperature and SWC and these are also interrelated. Therefore, more research in the application of these models in others semi-arid systems is necessary. Despite that, when a multi-chamber system is not

available, we recommend for this type of ecosystem the use of daytime models in cold seasons and the use of nighttime models

430 in hot seasons when most of the contribution to R_s comes from the heterotrophic respiration of the alleys.

4.3 R_s drivers

Q_{10} differs in the alley and tree-base in terms of magnitude and seasonal evolution (Fig. 5). In the alley $Q_{10} > 1$ was always found, but under the canopy, we found periods with Q_{10} values close to 1. This means that the variation in R_s during this period is decoupled from changes in soil temperature. In addition, $Q_{10} < 1$ values during summer indicated that respiration 435 decreased as temperature increased. That is, the respiration of the under-tree rooting zone of the tree canopy was associated with soil temperature. Therefore, the traditional parameter Q_{10} , determined through field measurements of R_s and temperature (Davidson and Janssens, 2006) cannot be used to define the respiration of Mediterranean ecosystems because of their large spatial and temporal heterogeneity where there are plants that inhibit their respiration at high temperatures. The Q_{10} values obtained in this study were calculated using 7-day windows and soil temperature measurements at a depth of 5 cm. However, 440 these results may vary depending on the length of the time window and the depth of the temperature sensors, as the temperature propagation through the soil introduces a time lag that can influence the estimates (Barron-Gafford et al., 2011; Hamerlynck et al., 2013). It is currently known that variations in Q_{10} are controlled by soil and vegetation factors and not only climate (Chen et al., 2020). Therefore, although the global value of Q_{10} is estimated to be 1.5 (Bond-Lamberty and Thomson, 2010), the variability of reported Q_{10} varies enormously, reaching values higher than 200 in ecosystems with very low temperatures 445 (Mikan et al., 2002). Conversely, Q_{10} values less than 1 have been found in other regions with semi-arid climates that include a dry period such as continental monsoon (Han and Jin, 2018), suggesting that it is not exclusively found in olive groves, but may be common in water-limited ecosystems with dry periods. In addition, the regressions used to obtain Q_{10} are usually not good when the water content in the soil is low (Wang et al., 2014) and the R_s - T_{soil} relationship disappears or even becomes negative as we can see in figure 5.

450 The areas with the greatest uncertainty in global R_s prediction models are semi-arid regions (Warner et al., 2019), where water acts as a limiting factor and R_s decreases even with increasing temperature (Zhao et al., 2017). For example, in Mediterranean mountain grasslands, temperature is no longer a good predictor (Bahn et al., 2008). In our study, we observed a coincidence in the alley of the reduction of R_s with the prolonged decrease in soil moisture in the prolonged summer drought (July - September), indicating a connection between R_s and humidity (Fig. 3). Thus, even if the temperature increases in July, R_s in

455 the two locations appears to decrease. However, $R_{s-Under-Tree}$ also decreased with the advance of summer even though $SWC_{Under-Tree}$ remained relatively constant due to irrigation. Also, $R_{s-Under-Tree}$ was practically constant throughout the day except in summer when there is a negative relationship with temperature. This decoupling could be explained by a reduction of root exudates due to reduced photosynthesis of olive trees that could be induced by an increase in VPD. It is known that tree photosynthesis modulates soil respiration (Högberg et al., 2001) as metabolic activity is related to the closure of stomata at 460 high temperatures (Tang et al., 2005; Makita et al., 2018). CO_2 assimilation decreases with high VPD values when olive trees

close their stomata (Fernández and Moreno, 1999), affecting the NEE (Chamizo et al., 2017). Here, we have observed that GPP values also decrease with soil temperature in the summer months (data not shown). However, we also observed negative Ts and Rs ratios at night so this mechanism could have a delay of hours or there may be additional mechanisms that we cannot elucidate. Stomatal closure has an impact on the rhizosphere because it inhibits the transport of photosynthetic products or carbohydrates from photosynthesis (which in turn depends on ecophysiological and meteorological factors) by the phloem, decreasing root activity and exudates, thus decreasing under-tree rooting zone respiration (R_z). Therefore, R_z may be dynamically linked to vegetative growth, climate, or competition, all linked to CO_2 assimilation capacity of olive trees (Aranda-Barranco et al., 2023). Tang et al. (2005) established that the translocation time of photosynthetic products from leaves to roots can be between 7 and 12 h. The lag for the isotopic signal of photosynthesis in trees to appear at R_s is in the range of days in other ecosystems (Ekblad and Högberg, 2001), which seems to indicate that stomatal closure would have an immediate effect (hours) on the reduction in CO_2 transport to the rhizosphere, whereas it would have a later effect (days) on the reduction of root exudates. The reduction in R_s at high VPD values is observed both at night and during the day and at times with and without irrigation. Nevertheless, the association between photosynthesis and R_s – Under-Tree can be confused with the relationship between T_s and R_s and more study is needed in this regard to establish the connection between VPD and R_z .

475 Therefore, the response of R_s to temperature fluctuations is influenced not only by soil temperature, making it crucial to consider additional factors such as SWC, photosynthesis, or precipitation events when modeling R_s in Mediterranean environments (González-Ubierna and Lai, 2019). In our study, we see that the variations of SWC are higher in the alleys (Fig. S2a); therefore, the variability of the relationship between R_s and T_s will be higher if they are conditioned by humidity. In addition, the drivers are interrelated as temperature-dependent responses that are further influenced by soil moisture and 480 precipitation (Hursh et al., 2017). Furthermore, we identified hysteresis behavior only in summer in alleys, which could indicate diurnal changes of SWC close to some critical value for the R_s/T_{soil} relation. However, finding the hysteresis pattern also with SWC indicates that there is another factor in addition to temperature involved in R_s .

4.4 Rain Pulse Events

Although the main transport process is molecular diffusion, rain pulse events can also produce an immediate release 485 of CO_2 by displacing gas within the pores (Inglima et al., 2009). Marañón-Jiménez et al. (2011) suggest that a significant portion of the CO_2 released within the first two hours after water is added likely originates from the degassing of CO_2 -rich air trapped in the soil pores. CO_2 adsorbed to the surface of soil particles (Ravikovitch et al., 2005) and stimulation of microbial activity can increase soil respiration (Jarvis et al., 2007). Rain pulses can be the most important driver in terms of the seasonal trend of soil CO_2 efflux in semi-arid ecosystems (Leon et al., 2014). We can see that water is a limiting factor for R_s with a 490 large rainfall pulse after the summer drought (first rectangle on the left; Fig. 3); however, in periods with high SWC, this relationship is lost (Fig. 7b). Other studies in olive grove alleys (Testi et al., 2008; Sierra et al., 2016; Chamizo et al., 2017) have shown R_s values between $0.5\text{--}1.6 \mu\text{mol m}^{-2} \text{s}^{-1}$ ($n_{\text{collar}} \sim 10$) based on field campaign measurements taken outside of rainy

days. In contrast, using automatic measurements, we found a higher variability with $0.4 - 11.3 \mu\text{mol m}^2 \text{s}^{-1}$ values ($n = 365$), but with a median of $1.5 \mu\text{mol m}^2 \text{s}^{-1}$ (Fig. 2a), within the range of the other studies. This reflects the fact that continuous measurements can detect rain pulse events that tend to fall outside the usual ranges. The conventional daytime and nighttime methods for R_{eco} partitioning via Eddy covariance data modeling appear not to respond to rainfall pulses, whether the soil was previously dry or not (Fig. 8d), and this becomes evident when we observe how only the chamber fluxes respond to a PPT event.

In our study, pulses of rain were detected on 11% of the days of the year, which implied that up to 18% of CO_2 emissions occurred on days with pulses of rain which implied that 15% of $R_{s,\text{eco}}$ emissions came from rain pulses. However, the variability in pulse length was high, with pulses lasting between the high intensity moment of the first hour and up to several days. Given that the duration of the pulses is usually between 3 and 6 h at our site and the intensity of rain pulse events decreases with successive events, we can be more cautious and estimate that the total ecosystem contribution of rain pulses is less than 15%, as is the case of others semi-arid areas (Delgado-Balbuena et al., 2023) where 5% contribution was estimated. At the ecosystem scale, we observed slight pulse signals with a lag of several days; therefore, the NEE models based exclusively on radiation or temperature may not be the most accurate for real-time characterization of this phenomenon. However, incorporating soil water content into these models would significantly enhance their predictive ability for the Birch effect.

The effect of rain pulse events on R_s is spatially dependent in agrosystems with two vegetation levels. The rain pulse events were higher with greater time elapsed since the last rain episode confirming that mineralization falls off in successive cycles as the amount of carbon declines (Birch, 1964), but this relationship was only described in the alleys (Fig. 8), whereas the rain pulse events under the tree were less noticeable (Fig. 7b and Fig. 7c) with low r and p values. This could be because i) the rain pulse events are higher in drier soils (Morillas et al., 2017), so the pulses may be less noticeable in irrigated areas, ii) the rain pulses are inhibited by the tree canopy, implying rain interception (in fact, we can see lower ΔSWC in rainy episodes under-tree) iii) This process is more difficult to observe when soil respiration is largely autotrophic as the Birch effect primarily involves heterotrophic respiration (Birch, 1964) or iv) the carbon supply and the different soil characteristics lead to different CO_2 release responses (Barnard et al., 2020). Rainfall pulses are reduced when vegetation cover is present (Liang et al., 2023) because the intensity of the event on the ground decreases and because soil respiration rates in grasslands typically decline after multiple rewetting cycles (Fierer and Schimel, 2002). Also, porosity may be greater in the alleys since the usual treatment before starting to apply herbicide in 2014 was the establishment of a vegetal cover which can increase porosity (Basche & DeLonge, 2017) and therefore volumetric displacement (Marañón-Jiménez et al., 2011). In general, this region shows a paradoxical increase in extreme precipitation events, even as the total annual amount decreases (Zittis et al., 2021). Therefore, this phenomenon of releasing CO_2 could gain importance in the future in Mediterranean ecosystems. The implications of different management regimes in Mediterranean agroecosystems could be crucial for climate change mitigation strategies as they could lead to R_s reductions (Wollenberg et al., 2016; Montanaro et al., 2023) with the use of covers that reduce losses of CO_2 from precipitation events.

5. Conclusions

Continuous measurement with a multi-chamber system revealed a higher range of soil respiration (R_s) values than those previously reported in olive groves. R_s - Under Tree was on average 3 times higher than R_s - Alley, especially in the cold months when 50% of R_s at the ecosystem level came from R_s - Under Tree, even though the canopy fraction represents only 27%. Therefore, it cannot be assumed that R_s - Alley is representative of olive grove soil respiration. Also, consistent patterns showing higher R_s on the south side of the tree individuals and exponential decrease from the trees to the alley center allowed us to calculate the accumulated R_s at the ecosystem level.

The annual accumulation was 2100 g C m⁻² and twice the ecosystem respiration (R_{eco}) obtained from eddy covariance. The higher the role of tree respiration on the R_s of the ecosystem, the worse the relationship between the R_s behavior of the chambers and the modeled R_{eco-NT} , showing that temperature-based models are insufficient in olive groves in cold months. Furthermore, inverse relationships between R_s and temperature were found in summer (Q_{10} less than 1), indicating that the variation of R_s during this period is decoupled from changes in soil temperature. Although the process needs to be studied in more depth, it could be related to a reduce in newly produced photosynthates given a high VPD since GPP also decreased with soil temperature in summer

Finally, large pulses of CO₂ were observed when rain fell on dry soil and were higher with longer rain-free periods. The tree structure reduced the relationship and magnitude of the pulses with precipitation, thus reflecting interception. The pulses were determined by the previous soil moisture conditions, and the detection of the pulses was lost when aboveground respiration and soil respiration was observed together with eddy covariance. The continuity of the measurements allowed clear spatial differences to be established in the response of R_s to changes in temperature, soil moisture, and rainfall pulses. All these findings show spatial and temporal variability in R_s and its drivers that should be considered in future studies of soil CO₂ respiration in Mediterranean agrosystems.

Declaration of Competing Interest

The authors declare that they have no known competing financial interests or personal relationships that could have appeared to influence the work reported in this paper.

550 Acknowledgments

This work was supported by the Spanish Ministry of Science and Innovation through projects CGL2017- 83538-471 C3- 1- R (ELEMENTAL) including European Union ERDF funds [grant number PRE2018-085638], the PID2020-117825GB-C21 and PID2020-117825GB-C22 (INTEGRATYON3) and the projects ICAERSA (P18-RT-3629), OLEAGEIs (B-RNM-60-UGR20) and MORADO (C-EXP-366-UGR23) funded by the Andalusian regional government and the European Union including

555 European Funds for Regional Development. A-B. S acknowledges support from the FPU grant by the Ministry of Universities
of Spain. [REF:]. FPU19/01647. Thanks are given to the Group of Castillo de Canena for the use of their farm as an
experimental site and their people for continuous cooperation and to Manuel Martos for collecting data in the manual
campaigns with the portable chamber. We appreciate Elise Pendall's comments in the review process

References

560 Almagro, M., López, J., Querejeta, J. I., and Martínez-Mena, M.: Temperature dependence of soil CO₂ efflux is strongly
modulated by seasonal patterns of moisture availability in a Mediterranean ecosystem, *Soil Biol. Biochem.*, 41,
<https://doi.org/10.1016/j.soilbio.2008.12.021>, 2009.

Álvarez, S., Soriano, M. A., Landa, B. B., and Gómez, J. A.: Soil properties in organic olive groves compared with that in
natural areas in a mountainous landscape in southern Spain, *Soil Use Manag.*, 23, <https://doi.org/10.1111/j.1475-2743.2007.00104.x>, 2007.

565 Aranda-Barranco, S., Serrano-Ortiz, P., Kowalski, A. S., and Sánchez-Cañete, E. P.: The temporary effect of weed-cover
maintenance on transpiration and carbon assimilation of olive trees, *Agric. For. Meteorol.*, 329, 109266,
<https://doi.org/10.1016/j.agrformet.2022.109266>, 2023.

Bahn, M., Rodeghiero, M., Anderson-Dunn, M., Dore, S., Gimeno, C., Drösler, M., Williams, M., Ammann, C., Berninger,
570 Flechard, C., Jones, S., Balzarolo, M., Kumar, S., Newesely, C., Priwitzer, T., Raschi, A., Siegwolf, R., Susiluoto, S.,
Tenhunen, J., Wohlfahrt, G., and Cernusca, A.: Soil respiration in European grasslands in relation to climate and assimilate
supply, *Ecosystems*, 11, <https://doi.org/10.1007/s10021-008-9198-0>, 2008.

Baldocchi, D. D.: How eddy covariance flux measurements have contributed to our understanding of Global Change Biology,
<https://doi.org/10.1111/gcb.14807>, 2020.

575 Barnard, R. L., Blazewicz, S. J., and Firestone, M. K.: Rewetting of soil: Revisiting the origin of soil CO₂ emissions,
<https://doi.org/10.1016/j.soilbio.2020.107819>, 2020.

Barron-Gafford, G. A., Scott, R. L., Jenerette, G. D., and Huxman, T. E.: The relative controls of temperature, soil moisture,
and plant functional group on soil CO₂ efflux at diel, seasonal, and annual scales, *J. Geophys. Res. Biogeosciences*, 116,
<https://doi.org/10.1029/2010JG001442>, 2011.

580 Basche, A., & DeLonge, M: The Impact of Continuous Living Cover on Soil Hydrologic Properties: A Meta-Analysis. *Soil
Science Society of America Journal*. <https://doi.org/10.2136/sssaj2017.03.0077>, 2017

Bertolla, C., Caruso, G., and Gucci, R.: Seasonal changes in soil respiration rates in olive orchards, *Acta Hortic.*,
<https://doi.org/10.17660/ActaHortic.2014.1057.30>, 2014.

Birch, H. F.: Mineralisation of plant nitrogen following alternate wet and dry conditions, *Plant Soil*, 20,
585 <https://doi.org/10.1007/BF01378096>, 1964.

Bond-Lamberty, B. and Thomson, A.: Temperature-associated increases in the global soil respiration record, *Nature*, 464,

https://doi.org/10.1038/nature08930, 2010.

Chamizo, S., Serrano-Ortiz, P., López-Ballesteros, A., Sánchez-Cañete, E. P., Vicente-Vicente, J. L., and Kowalski, A. S.: Net ecosystem CO₂exchange in an irrigated olive orchard of SE Spain: Influence of weed cover, *Agric. Ecosyst. Environ.*, 239, 51–64, <https://doi.org/10.1016/j.agee.2017.01.016>, 2017.

590 Chen, S., Wang, J., Zhang, T., and Hu, Z.: Climatic, soil, and vegetation controls of the temperature sensitivity (Q10) of soil respiration across terrestrial biomes, *Glob. Ecol. Conserv.*, 22, <https://doi.org/10.1016/j.gecco.2020.e00955>, 2020.

Comeau, L. P., Lai, D. Y. F., Jinglan Cui, J., and Farmer, J.: Separation of soil respiration: A site-specific comparison of partition methods, in: *SOIL*, <https://doi.org/10.5194/soil-4-141-2018>, 2018.

595 Davidson, E. A. and Janssens, I. A.: Temperature sensitivity of soil carbon decomposition and feedbacks to climate change, <https://doi.org/10.1038/nature04514>, 2006.

Delgado-Balbuena, J., Loescher, H. W., Aguirre-Gutiérrez, C. A., Alfaro-Reyna, T., Pineda-Martínez, L. F., Vargas, R., and Arredondo, T.: Dynamics of short-term ecosystem carbon fluxes induced by precipitation events in a semiarid grassland, *Biogeosciences*, 20, <https://doi.org/10.5194/bg-20-2369-2023>, 2023.

600 Ekblad, A. and Högberg, P.: Natural abundance of ¹³C in CO₂ respired from forest soils reveals speed of link between tree photosynthesis and root respiration, *Oecologia*, 127, <https://doi.org/10.1007/s004420100667>, 2001.

FAOSTAT (September 9, 2023). Food and Agriculture Organization of the United Nations Statistical Dataset. Obtained from: <https://www.fao.org/faostat/en/#data>

Fernández, J. E. and Moreno, F.: Water use by the olive tree, https://doi.org/10.1300/J144v02n02_05, 1999.

605 Fierer, N. and Schimel, J. P.: Effects of drying-rewetting frequency on soil carbon and nitrogen transformations, *Soil Biol. Biochem.*, 34, [https://doi.org/10.1016/S0038-0717\(02\)00007-X](https://doi.org/10.1016/S0038-0717(02)00007-X), 2002.

Fratini, G., Ibrom, A., Arriga, N., Burba, G., and Papale, D.: Relative humidity effects on water vapour fluxes measured with closed-path eddy-covariance systems with short sampling lines, *Agric. For. Meteorol.*, <https://doi.org/10.1016/j.agrformet.2012.05.018>, 2012.

610 Friedlingstein, P., O'sullivan, M., Jones, M. W., Andrew, R. M., Gregor, L., Hauck, J., Le Quéré, C., Luijkx, I. T., Olsen, A., Peters, G. P., Peters, W., Pongratz, J., Schwingshackl, C., Sitch, S., Canadell, J. G., Ciais, P., Jackson, R. B., Alin, S. R., Alkama, R., Arneth, A., Arora, V. K., Bates, N. R., Becker, M., Bellouin, N., Bittig, H. C., Bopp, L., Chevallier, F., Chini, L. P., Cronin, M., Evans, W., Falk, S., Feely, R. A., Gasser, T., Gehlen, M., Gkritzalis, T., Gloege, L., Grassi, G., Gruber, N., Gürses, Ö., Harris, I., Hefner, M., Houghton, R. A., Hurt, G. C., Iida, Y., Ilyina, T., Jain, A. K., Jersild, A., Kadono, K., Kato, E., Kennedy, D., Klein Goldewijk, K., Knauer, J., Korsbakken, J. I., Landschützer, P., Lefèvre, N., Lindsay, K., Liu, J., Liu, Z., Marland, G., Mayot, N., McGrath, M. J., Metzl, N., Monacci, N. M., Munro, D. R., Nakaoka, S. I., Niwa, Y., O'brien, K., Ono, T., Palmer, P. I., Pan, N., Pierrot, D., Pocock, K., Poulter, B., Resplandy, L., Robertson, E., Rödenbeck, C., Rodriguez, C., Rosan, T. M., Schwinger, J., Séférian, R., Shutler, J. D., Skjelvan, I., Steinhoff, T., Sun, Q., Sutton, A. J., Sweeney, C., Takao, S., Tanhua, T., Tans, P. P., Tian, X., Tian, H., Tilbrook, B., Tsujino, H., Tubiello, F., Van Der Werf, G. R., Walker, A.

615 620 P., Wanninkhof, R., Whitehead, C., Willstrand Wranne, A., et al.: Global Carbon Budget 2022, *Earth Syst. Sci. Data*, 14,

<https://doi.org/10.5194/essd-14-4811-2022>, 2022.

García-Ruiz, J. M., Nadal-Romero, E., Lana-Renault, N., and Beguería, S.: Erosion in Mediterranean landscapes: Changes and future challenges, <https://doi.org/10.1016/j.geomorph.2013.05.023>, 2013.

625 Gómez, J. A., Sobrinho, T. A., Giráldez, J. V., and Fereres, E.: Soil management effects on runoff, erosion and soil properties in an olive grove of Southern Spain, *Soil Tillage Res.*, 102, 5–13, <https://doi.org/10.1016/j.still.2008.05.005>, 2009.

González-Ubierna, S. and Lai, R.: Modelling the effects of climate factors on soil respiration across Mediterranean ecosystems, *J. Arid Environ.*, 165, <https://doi.org/10.1016/j.jaridenv.2019.02.008>, 2019.

630 Hamerlynck, E. P., Scott, R. L., Sánchez-Cañete, E. P., and Barron-Gafford, G. A.: Nocturnal soil CO₂ uptake and its relationship to subsurface soil and ecosystem carbon fluxes in a Chihuahuan Desert shrubland, *J. Geophys. Res. Biogeosciences*, 118, <https://doi.org/10.1002/2013JG002495>, 2013.

Han, M. and Jin, G.: Seasonal variations of Q10 soil respiration and its components in the temperate forest ecosystems, northeastern China, *Eur. J. Soil Biol.*, 85, <https://doi.org/10.1016/j.ejsobi.2018.01.001>, 2018.

Hashimoto, S., Carvalhais, N., Ito, A., Migliavacca, M., Nishina, K., and Reichstein, M.: Global spatiotemporal distribution of soil respiration modeled using a global database, *Biogeosciences*, 12, <https://doi.org/10.5194/bg-12-4121-2015>, 2015.

635 Högberg, P., Nordgren, A., Buchmann, N., Taylor, A. F. S., Ekblad, A., Högberg, M. N., Nyberg, G., Ottosson-Löfvenius, M., and Read, D. J.: Large-scale forest girdling shows that current photosynthesis drives soil respiration, *Nature*, 411, <https://doi.org/10.1038/35081058>, 2001.

Hursh, A., Ballantyne, A., Cooper, L., Maneta, M., Kimball, J., and Watts, J.: The sensitivity of soil respiration to soil temperature, moisture, and carbon supply at the global scale, *Glob. Chang. Biol.*, 23, <https://doi.org/10.1111/gcb.13489>, 2017.

640 IFAPA. (March 17, 2022). Instituto Andaluz de Investigación y Formación Agraria, Pesquera, Alimentaria y de la Producción Ecológica (IFAPA). Estaciones Agroclimáticas. Obtained from:

<https://www.juntadeandalucia.es/agriculturaypesca/ifapa/ria/servlet/FrontController>.

645 Inglima, I., Alberti, G., Bertolini, T., Vaccari, F. P., Gioli, B., Miglietta, F., Cotrufo, M. F., and Peressotti, A.: Precipitation pulses enhance respiration of Mediterranean ecosystems: The balance between organic and inorganic components of increased soil CO₂ efflux, *Glob. Chang. Biol.*, 15, <https://doi.org/10.1111/j.1365-2486.2008.01793.x>, 2009.

Jarvis, P., Rey, A., Petsikos, C., Wingate, L., Rayment, M., Pereira, J., Banza, J., David, J., Miglietta, F., Borghetti, M., Manca, G., and Valentini, R.: Drying and wetting of Mediterranean soils stimulates decomposition and carbon dioxide emission: The “Birch effect,” in: *Tree Physiology*, <https://doi.org/10.1093/treephys/27.7.929>, 2007.

650 Jian, J., Vargas, R., Anderson-Teixeira, K., Stell, E., Herrmann, V., Horn, M., Kholod, N., Manzon, J., Marchesi, R., Paredes, D., and Bond-Lamberty, B.: A restructured and updated global soil respiration database (SRDB-V5), *Earth Syst. Sci. Data*, 13, <https://doi.org/10.5194/essd-13-255-2021>, 2021.

Kutikoff, S., Lin, X., Evett, S. R., Gowda, P., Brauer, D., Moorhead, J., Marek, G., Colaizzi, P., Aiken, R., Xu, L., and Owensby, C.: Water vapor density and turbulent fluxes from three generations of infrared gas analyzers, *Atmos. Meas. Tech.*, 14, 1253–1266, <https://doi.org/10.5194/amt-14-1253-2021>, 2021.

655 Lasslop, G., Reichstein, M., Papale, D., Richardson, A., Arneth, A., Barr, A., Stoy, P., and Wohlfahrt, G.: Separation of net ecosystem exchange into assimilation and respiration using a light response curve approach: Critical issues and global evaluation, *Glob. Chang. Biol.*, <https://doi.org/10.1111/j.1365-2486.2009.02041.x>, 2010.

Lei, J., Guo, X., Zeng, Y., Zhou, J., Gao, Q., and Yang, Y.: Temporal changes in global soil respiration since 1987, *Nat. Commun.*, 12, <https://doi.org/10.1038/s41467-020-20616-z>, 2021.

660 Leon, E., Vargas, R., Bullock, S., Lopez, E., Panosso, A. R., and La Scala, N.: Hot spots, hot moments, and spatio-temporal controls on soil CO₂ efflux in a water-limited ecosystem, *Soil Biol. Biochem.*, 77, <https://doi.org/10.1016/j.soilbio.2014.05.029>, 2014.

Li, J., Pei, J., Pendall, E., Fang, C., and Nie, M.: Spatial heterogeneity of temperature sensitivity of soil respiration: A global analysis of field observations, *Soil Biol. Biochem.*, 141, <https://doi.org/10.1016/j.soilbio.2019.107675>, 2020.

665 Liang, Z., Rasmussen, J., Poeplau, C., and Elsgaard, L.: Priming effects decrease with the quantity of cover crop residues – Potential implications for soil carbon sequestration, *Soil Biol. Biochem.*, 184, <https://doi.org/10.1016/j.soilbio.2023.109110>, 2023.

Lloyd, J. and Taylor, J. A.: On the Temperature Dependence of Soil Respiration, *Funct. Ecol.*, 8, <https://doi.org/10.2307/2389824>, 1994.

670 Makita, N., Kosugi, Y., Sakabe, A., Kanazawa, A., Ohkubo, S., and Tani, M.: Seasonal and diurnal patterns of soil respiration in an evergreen coniferous forest: Evidence from six years of observation with automatic chambers, *PLoS One*, 13, <https://doi.org/10.1371/journal.pone.0192622>, 2018.

Malek, Ž. and Verburg, P.: Mediterranean land systems: Representing diversity and intensity of complex land systems in a dynamic region, *Landsc. Urban Plan.*, 165, <https://doi.org/10.1016/j.landurbplan.2017.05.012>, 2017.

675 Marañón-Jiménez, S., Castro, J., Kowalski, A. S., Serrano-Ortiz, P., Reverter, B. R., Sánchez-Cañete, E. P., and Zamora, R.: Post-fire soil respiration in relation to burnt wood management in a Mediterranean mountain ecosystem, *For. Ecol. Manage.*, 261, 1436–1447, <https://doi.org/10.1016/j.foreco.2011.01.030>, 2011.

Marzaioli, R., D'Ascoli, R., De Pascale, R. A., and Rutigliano, F. A.: Soil quality in a Mediterranean area of Southern Italy as related to different land use types, *Appl. Soil Ecol.*, 44, <https://doi.org/10.1016/j.apsoil.2009.12.007>, 2010.

680 Mauder, M., Cuntz, M., Drüe, C., Graf, A., Rebmann, C., Schmid, H. P., Schmidt, M., and Steinbrecher, R.: A strategy for quality and uncertainty assessment of long-term eddy-covariance measurements, *Agric. For. Meteorol.*, 169, <https://doi.org/10.1016/j.agrformet.2012.09.006>, 2013.

Mikan, C. J., Schimel, J. P., and Doyle, A. P.: Temperature controls of microbial respiration in arctic tundra soils above and below freezing, *Soil Biol. Biochem.*, 34, [https://doi.org/10.1016/S0038-0717\(02\)00168-2](https://doi.org/10.1016/S0038-0717(02)00168-2), 2002.

685 Moncrieff, J., Clement, R., Finnigan, J., and Meyers, T.: Averaging, Detrending, and Filtering of Eddy Covariance Time Series, in: *Handbook of Micrometeorology*, https://doi.org/10.1007/1-4020-2265-4_2, 2006.

Montanaro, G., Doupis, G., Kourgialas, N., Markakis, E., Kavroulakis, N., Psarras, G., Koubouris, G., Dichio, B., and Nuzzo, V.: Management options influence seasonal CO₂ soil emissions in Mediterranean olive ecosystems, *Eur. J. Agron.*, 146,

<https://doi.org/10.1016/j.eja.2023.126815>, 2023.

690 Moriana, A., Orgaz, F., Pastor, M., and Fereres, E.: Yield responses of a mature olive orchard to water deficits, *J. Am. Soc. Hortic. Sci.*, <https://doi.org/10.21273/jashs.128.3.0425>, 2003.

Morillas, L., Roales, J., Portillo-Estrada, M., and Gallardo, A.: Wetting-drying cycles influence on soil respiration in two Mediterranean ecosystems, *Eur. J. Soil Biol.*, 82, <https://doi.org/10.1016/j.ejsobi.2017.07.002>, 2017.

Munoz-Rojas, M., Jordan, A., Zavala, L. M., De La Rosa, D., Abd-Elmabod, S. K., and Anaya-Romero, M.: Organic carbon stocks in Mediterranean soil types under different land uses (Southern Spain), *Solid Earth*, 3, <https://doi.org/10.5194/se-3-375-2012>, 2012.

Nieto, O. M., Castro, J., and Fernández-Ondoño, E.: Conventional tillage versus cover crops in relation to carbon fixation in Mediterranean olive cultivation, *Plant Soil*, 365, 321–335, <https://doi.org/10.1007/s11104-012-1395-0>, 2013.

700 Novara, A., Cerdà, A., Barone, E., and Gristina, L.: Cover crop management and water conservation in vineyard and olive orchards, <https://doi.org/10.1016/j.still.2020.104896>, 2021.

Panettieri, M., Moreno, B., de Sosa, L. L., Benítez, E., and Madejón, E.: Soil management and compost amendment are the main drivers of carbon sequestration in rainfed olive trees agroecosystems: An evaluation of chemical and biological markers, *Catena*, 214, <https://doi.org/10.1016/j.catena.2022.106258>, 2022.

Ravikovitch, P. I., Bogan, B. W., and Neimark, A. V.: Nitrogen and carbon dioxide adsorption by soils, *Environ. Sci. Technol.*, 39, <https://doi.org/10.1021/es048307b>, 2005.

705 Reichstein, M., Falge, E., Baldocchi, D., Papale, D., Aubinet, M., Berbigier, P., Bernhofer, C., Buchmann, N., Gilmanov, T., Granier, A., Grünwald, T., Havránková, K., Ilvesniemi, H., Janous, D., Knohl, A., Laurila, T., Lohila, A., Loustau, D., Matteucci, G., Meyers, T., Miglietta, F., Ourcival, J. M., Pumpanen, J., Rambal, S., Rotenberg, E., Sanz, M., Tenhunen, J., Seufert, G., Vaccari, F., Vesala, T., Yakir, D., and Valentini, R.: On the separation of net ecosystem exchange into assimilation and ecosystem respiration: Review and improved algorithm, <https://doi.org/10.1111/j.1365-2486.2005.001002.x>, 2005.

Sánchez-Cañete, E. P., Scott, R. L., van Haren, J., and Barron-Gafford, G. A.: Improving the accuracy of the gradient method for determining soil carbon dioxide efflux, *J. Geophys. Res. Biogeosciences*, 122, <https://doi.org/10.1002/2016JG003530>, 2017.

710 SIERRA, M., MARTÍNEZ, F. J., BRAJOS, V., ROMERO-FREIRE, A., ORTIZ-BERNAD, I., and MARTÍN, F. J.: Chemical stabilization of organic carbon in agricultural soils in a semi-arid region (SE Spain), *J. Agric. Sci.*, 154, 87–97, <https://doi.org/10.1017/S002185961500012X>, 2016.

Skopp, J., Jawson, M. D., and Doran, J. W.: Steady-State Aerobic Microbial Activity as a Function of Soil Water Content, *Soil Sci. Soc. Am. J.*, 54, <https://doi.org/10.2136/sssaj1990.03615995005400060018x>, 1990.

720 Stoyan, H., De-Polli, H., Böhm, S., Robertson, G. P., and Paul, E. A.: Spatial heterogeneity of soil respiration and related properties at the plant scale, *Plant Soil*, 222, <https://doi.org/10.1023/a:1004757405147>, 2000.

Taguas, E. V., Marín-Moreno, V., Díez, C. M., Mateos, L., Barranco, D., Mesas-Carrascosa, F. J., Pérez, R., García-Ferrer, A., and Quero, J. L.: Opportunities of super high-density olive orchard to improve soil quality: Management guidelines for

application of pruning residues, *J. Environ. Manage.*, 293, <https://doi.org/10.1016/j.jenvman.2021.112785>, 2021.

Talmon, Y., Sternberg, M., and Grünzweig, J. M.: Impact of rainfall manipulations and biotic controls on soil respiration in
725 Mediterranean and desert ecosystems along an aridity gradient, *Glob. Chang. Biol.*, 17, <https://doi.org/10.1111/j.1365-2486.2010.02285.x>, 2011.

Tang, J., Baldocchi, D. D., and Xu, L.: Tree photosynthesis modulates soil respiration on a diurnal time scale, *Glob. Chang. Biol.*, 11, <https://doi.org/10.1111/j.1365-2486.2005.00978.x>, 2005.

Testi, L., Orgaz, F., and Villalobos, F.: Carbon exchange and water use efficiency of a growing, irrigated olive orchard,
730 *Environ. Exp. Bot.*, <https://doi.org/10.1016/j.envexpbot.2007.11.006>, 2008.

Turrini, A., Caruso, G., Avio, L., Gennai, C., Palla, M., Agnolucci, M., Tomei, P. E., Giovannetti, M., and Gucci, R.: Protective green cover enhances soil respiration and native mycorrhizal potential compared with soil tillage in a high-density olive orchard in a long term study, *Appl. Soil Ecol.*, <https://doi.org/10.1016/j.apsoil.2017.04.001>, 2017.

Vargas, R. and Le, V. H.: The paradox of assessing greenhouse gases from soils for nature-based solutions, *Biogeosciences*,
735 20, 15–26, <https://doi.org/10.5194/bg-20-15-2023>, 2023.

Vickers, D. and Mahrt, L.: Quality control and flux sampling problems for tower and aircraft data, *J. Atmos. Ocean. Technol.*,
[https://doi.org/10.1175/1520-0426\(1997\)014<0512:QCAFSP>2.0.CO;2](https://doi.org/10.1175/1520-0426(1997)014<0512:QCAFSP>2.0.CO;2), 1997.

Wang, B., Zha, T. S., Jia, X., Wu, B., Zhang, Y. Q., and Qin, S. G.: Soil moisture modifies the response of soil respiration to temperature in a desert shrub ecosystem, *Biogeosciences*, 11, <https://doi.org/10.5194/bg-11-259-2014>, 2014.

740 Wang, Y., Luo, G., Li, C., Ye, H., Shi, H., Fan, B., Zhang, W., Zhang, C., Xie, M., and Zhang, Y.: Effects of land clearing for agriculture on soil organic carbon stocks in drylands: A meta-analysis, *Glob. Chang. Biol.*, 29, <https://doi.org/10.1111/gcb.16481>, 2023.

Warner, D. L., Bond-Lamberty, B., Jian, J., Stell, E., and Vargas, R.: Spatial Predictions and Associated Uncertainty of Annual Soil Respiration at the Global Scale, *Global Biogeochem. Cycles*, 33, <https://doi.org/10.1029/2019GB006264>, 2019.

745 Wollenberg, E., Richards, M., Smith, P., Havlík, P., Obersteiner, M., Tubiello, F. N., Herold, M., Gerber, P., Carter, S., Reisinger, A., van Vuuren, D. P., Dickie, A., Neufeldt, H., Sander, B. O., Wassmann, R., Sommer, R., Amonette, J. E., Falcucci, A., Herrero, M., Opio, C., Roman-Cuesta, R. M., Stehfest, E., Westhoek, H., Ortiz-Monasterio, I., Sapkota, T., Rufino, M. C., Thornton, P. K., Verchot, L., West, P. C., Soussana, J. F., Baedeker, T., Sadler, M., Vermeulen, S., and Campbell, B. M.: Reducing emissions from agriculture to meet the 2 °C target, *Glob. Chang. Biol.*, 22, <https://doi.org/10.1111/gcb.13340>, 2016.

Wutzler, T., Lucas-Moffat, A., Migliavacca, M., Knauer, J., Sickel, K., Šigut, L., Menzer, O., and Reichstein, M.: Basic and extensible post-processing of eddy covariance flux data with REddyProc, *Biogeosciences*, <https://doi.org/10.5194/bg-15-5015-2018>, 2018.

Xu, M. and Shang, H.: Contribution of soil respiration to the global carbon equation,
755 <https://doi.org/10.1016/j.jplph.2016.08.007>, 2016.

Zhao, Z., Peng, C., Yang, Q., Meng, F. R., Song, X., Chen, S., Epule, T. E., Li, P., and Zhu, Q.: Model prediction of biome-

specific global soil respiration from 1960 to 2012, *Earth's Futur.*, 5, <https://doi.org/10.1002/2016EF000480>, 2017.

Zittis, G., Bruggeman, A., and Lelieveld, J.: Revisiting future extreme precipitation trends in the Mediterranean, *Weather Clim. Extrem.*, 34, <https://doi.org/10.1016/j.wace.2021.100380>, 2021.